White Matter Lesions in Adults – a Differential Diagnostic Approach

Läsionen der weißen Substanz im Erwachsenenalter – ein differenzialdiagnostischer Ansatz

Authors
Stefan Weidauer[1], Marlies Wagner[2], Elke Hattingen[2]

Affiliations
1 Neurology, Hospital of the Goethe University Frankfurt, Frankfurt am Main, Germany
2 Institute for Neuroradiology, Goethe University Frankfurt, Frankfurt am Main, Germany

Correspondence
Prof. Dr. Stefan Weidauer
Neurologische Klinik, St.-Katharinen-Krankenhaus,
Seckbacher Landstraße 65, 60389 Frankfurt, Germany
Tel.: ++ 49/69/46 03 15 30
Fax: ++ 49/69/46 03 15 29
stefan.weidauer@sankt-katharinen-ffm.de

ABSTRACT

Objective Cerebral white matter lesions on MRI in adults are a common finding. On the one hand, they may correspond to a clinically incidental feature, be physiologically or age-associated, or on the other hand they may be the overture to a severe neurological disease. With regard to pathophysiological aspects, practical hints for the differential diagnostic interpretation of lesions in daily clinical practice are presented.

Material and Methods With special regard to the vascular architecture and supply of the cerebral white matter, physiological structures are schematically represented and pathophysiological processes are highlighted by comparative image analysis of equally angulated MR sequences.

Results The most frequent vascular, inflammatory, metabolic, and neoplastic disease entities are presented on the basis of characteristic imaging findings and corresponding clinical- neurological constellations. The details of signal intensities and localization essential for differential diagnosis are highlighted.

Conclusion By means of comparative image analysis and the recognition of characteristic lesion patterns, taking into account anatomical principles and pathophysiological processes, the differential diagnostic classification of cerebral white matter lesions and associated diseases can be significantly facilitated. The additional consideration of clinical and laboratory findings is essential.

Key Points:
- Cerebral white matter lesions can be a harmless secondary finding or overture to a severe neurological disease.
- The comparative image analysis of different sequences with identical angulation is crucial.
- With special regard to the vascular anatomy, different lesion patterns can be identified.
- The consideration of neurological and laboratory chemical constellations is essential for the differential diagnosis.

Citation Format
- Weidauer S, Wagner M, Hattingen E. White Matter Lesions in Adults – a Differential Diagnostic Approach. Fortschr Röntgenstr 2020; 192: 1154–1173

ZUSAMMENFASSUNG

Ziel Zerebrale Marklagerläsionen im MRT beim Erwachsenen sind eine häufige Befundkonstellation. Sie können einerseits einem klinisch inapparenten Zufallsbefund entsprechen, physiologisch oder altersassoziiert sein, oder andererseits die Ouvertüre einer schweren neurologischen Erkrankung darstellen. Mit Bezug auf pathophysiologische Aspekte werden praktische Hinweise für die differenzialdiagnostische Läsionsinterpretation im klinischen Alltag aufgezeigt.

Material und Methode Unter besonderer Berücksichtigung der vaskulären Architektur und Versorgung des zerebralen Marklagers werden physiologische Strukturen schematisch dargestellt und pathophysiologische Vorgänge mittels vergleichender Bildanalyse von möglichst identisch angulierten MR-Sequenzen hervorgehoben.

Ergebnisse Anhand charakteristischer bildmorphologischer und klinisch-neurologischer Befundkonstellationen sind die wichtigsten und häufigsten vaskulären, entzündlichen, metabolischen und neoplastischen Krankheitsentitäten dargestellt und die für die differenzialdiagnostische Zuordnung essenziellen Details hinsichtlich Signalverhalten und Lokalisation hervorgehoben.

Schlussfolgerung Mittels vergleichender Bildanalyse und dem Erkennen charakteristischer Läsionsmuster unter Berücksichtigung anatomischer Grundlagen und pathophysiologischer Vorgänge kann die differenzialdiagnostische Zuordnung von Marklagererkrankungen wesentlich gebahnt werden. Essenziell ist der Einbezug klinischer und laborchemischer Befunde.

In adults, cerebral white matter lesions are a common MRI finding in the clinical routine [1, 2]. They can be either non-specific and age-related or indicative of the onset of severe neurological disease [1–4]. The image morphology is partially overlapping, with the hyperintense signal on the T2-weighted sequences (T2 WI) representing the common feature of these changes. Consequently, clinical-neurological data and laboratory chemical findings including CSF analysis are essential for differential diagnostic classification [1–6]. Furthermore, identified physiological constellations such as perivascular spaces must be distinguished [1, 7–10]. The etiology of white matter lesions is very heterogeneous and includes congenital [9], vascular [5, 7], inflammatory [11, 12], neoplastic [2, 5], neurodegenerative [2, 13, 14], metabolic [15–17], toxic [18–20] and traumatic origins. The resulting pathology includes cytotoxic and/or vasogenic edema, de- and remyelination, axonal lesions and hemorrhages with resulting necrosis, defects and gliosis [7, 11, 13, 21]. Characteristic lesion patterns should be recognized based on comparative image analysis of different identically angulated MRI sequences; based on clinical and laboratory chemical findings, these pave the way for differential diagnostic classification [1, 2, 5, 22]. The aim of this review is to explain diagnostic aspects of the classification of cerebral white matter lesions and to provide differential diagnostic tips with special regard to the vascular architecture of the white matter and pathological processes [6, 7, 10, 11].

Technical Aspects

The MR sequences listed in ► **Table 1** are necessary for the most reliable classification of white matter lesions. Diffusion tensor imaging (DTI), MR spectroscopy (MRS) and perfusion measurements are used as additional diagnostic tools, especially in cases of ambiguous diagnostic findings [1, 2, 5, 23]. Diffusion-weighted imaging (DWI) is acquired with diffusion gradients oriented in 3 orthogonal directions, which form the basis of directionally averaged DWI images (trace maps) [24]. The trace maps show the extent of diffusion of hydrogen protons, but not their directional dependence (anisotropy). The strength of diffusion weighting is described by the b-value [s/mm²], which is calculated from the properties of the diffusion gradients. Since the measured diffusion rates depend both on the chemical and physical tissue properties as well as the measurement conditions, the calculated diffusion values are referred to as apparent diffusion coefficient (ADC) [24]. Measurements with at least two different b-values are required to calculate ADC parameter images; b-values between 0 (pure T2-weighted image) and 1000 s/mm² are used for DWI measurements of the brain. Although two b-values are sufficient to create an ADC map, measurements with three b-values (b = 0, b = 500, b = 1000; each [s/mm²]) allow a more precise calculation of the ADC values. The lower signal-to-noise ratio (SNR) of the images with b = 1000 s/mm² leads to higher measurement inaccuracies, which are partly compensated by measurement with b = 500 s/mm². Compared to the ADC maps, the DWI images have the disadvantage that in the case of strongly T2-hyperintense changes on the DWI images, diffusion restriction is simulated (so-called "T2-shine through"), which is eliminated in the ADC maps [24].

In contrast to DWI, the DTI measures the anisotropy [25]. For this purpose, the diffusion images are measured with diffusion gradients oriented in at least 6 different spatial directions. Since the diffusion in the white matter through the fiber paths running in it is strongly directed along the fiber path, the parameters for the extent and direction of the anisotropy that can be calculated from the DTI are pathological early in most diseases of white matter [25].

In principle, 3D sequences offer the advantage of capturing small lesions more sensitively than 2D images with higher layer thickness because of the higher SNR, the high spatial resolution and the missing layer gaps [26]. In addition, 3D measurements in all planes can be reconstructed simply, curved multiplanar or as maximum intensity projection (MIP). A disadvantage compared to the 2D sequences is the usually longer measurement times with resulting motion sensitivity, whereas flow artifacts are usually more pronounced in 2D FLAIR (fluid attenuated inversion recovery) images than in the 3D images [26].

Vascular Anatomy of White Matter

1. Terminal pial and medullary arteries (4–5 cm long)

They originate from the three large leptomeningeal arteries (anterior, middle and posterior cerebral arteries) and move perpendicularly through the cortex into the white matter. Due to only a few capillary anastomoses, they represent functional end arteries (see ► **Fig. 1**) [7, 10, 27].

2. Subependymal arteries

These arise close to the ventricle from the choroidal arteries, which also extend perpendicularly into the deep white matter and are significantly shorter than the pial medullary vessels

3. End-arteries of the medial and lateral lenticulostriate and thalamic perforators

Due to only a few capillary anastomoses, they represent functional terminal arteries (see ► **Fig. 1**) [7, 10, 28]. Thus, the deep white

▶ **Table 1** MRI sequences.

weighting	geometry	sequence
T2	axial and sagittal[1] 2D	T2 spin echo (FSE, TSE)
	axial 2D, possibly sagittal 3D with axial reconstructions	FLAIR
diffusion	axial	DWI with 3 spatial directions and at least 2 b-values (0, 1000 s/mm²)
T1	axial	spin or gradient echo native, possibly also after IV administration of contrast[2]
	3D	TOF[3]
T2*	axial	SWI or T2 gradient echo

DWI: Diffusion-Weighted Imaging; FLAIR: Fluid Attenuated Inversion Recovery; FSE/TSE: Fast/Turbo Spin Echo; SWI: Susceptibility-Weighted Imaging; TOF: Time Of Flight.
[1] Especially helpful for the detection of corpus callosum lesions and pattern recognition.
[2] Intravenous administration of contrast medium is not routinely required, but depends on the pattern of lesions in the native T1 WI, taking into account the clinical symptoms and the specific issue.
[3] TOF-MRA sequences are T1-weighted. Thus, substances with short T1 times (hematoma, gadolinium, fat) can cause a "shine through" effect and simulate a flow signal, which can then be misinterpreted in MIP reconstructions as a flow signal or vessel malformation.
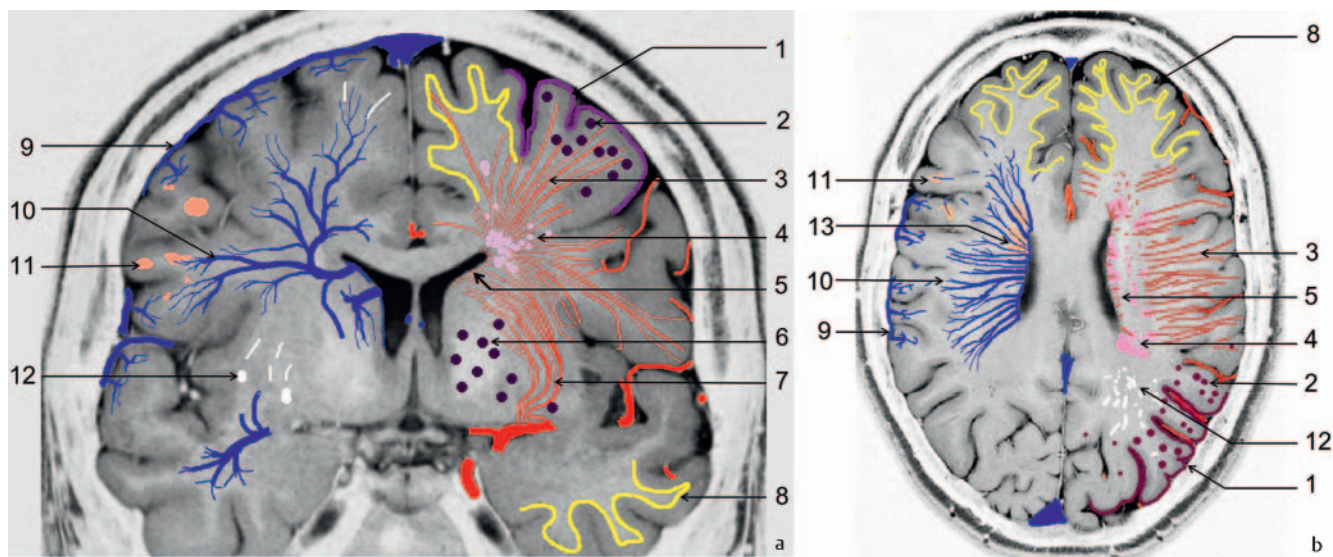
▶ **Fig. 1 a** Schematic representation of white matter lesions and vascular anatomy (coronal). 1: Superficial siderosis; 2: Cortical/subcortical microbleeds (MB); 3: Terminal pial and medullary arteries; 4: White matter changes (WMC); 5: Subependymal arteries; 6: Microbleeds (MB) in the basal ganglia and thalamus; 7: Medial and lateral lenticulostriate perforators; 8: U-fibres; 9: Superficial (cortical/leptomeningeal) veins; 10: Deep (internal) veins; 11: Cortical/juxtacortical MS plaques; 12: Dilated perivascular spaces (PVS). **b**: Schematic representation of white matter lesions and vascular anatomy (axial). 1: Superficial siderosis; 2: Cortical/subcortical microbleeds (MB) 3: Terminal pial and medullary arteries; 4: White matter changes (WMC); 5: Subependymal arteries; 8: U-fibres; 9: Superficial (cortical/leptomeningeal) veins; 10: Deep (internal) veins; 11: Cortical/juxtacortical MS plaques; 12: Dilated perivascular spaces (PVS); 13: Perivenular MS plaques with central vein (Dawson's finger).

matter is especially in the centrum semiovale and nearby the anterior horns border zone between superficial pial, deep subependymal and basal lenticulostriate and thalamo-perforating arteries [10]. This makes these deep white matter regions particularly vulnerable to vascular compromise (including "Steiner's Wetterwinkel"). In contrast, the juxtacortical region with the U-fibers is better vascularized than the deep white matter due to the cortical network of arterioles and numerous anastomoses [7, 10].
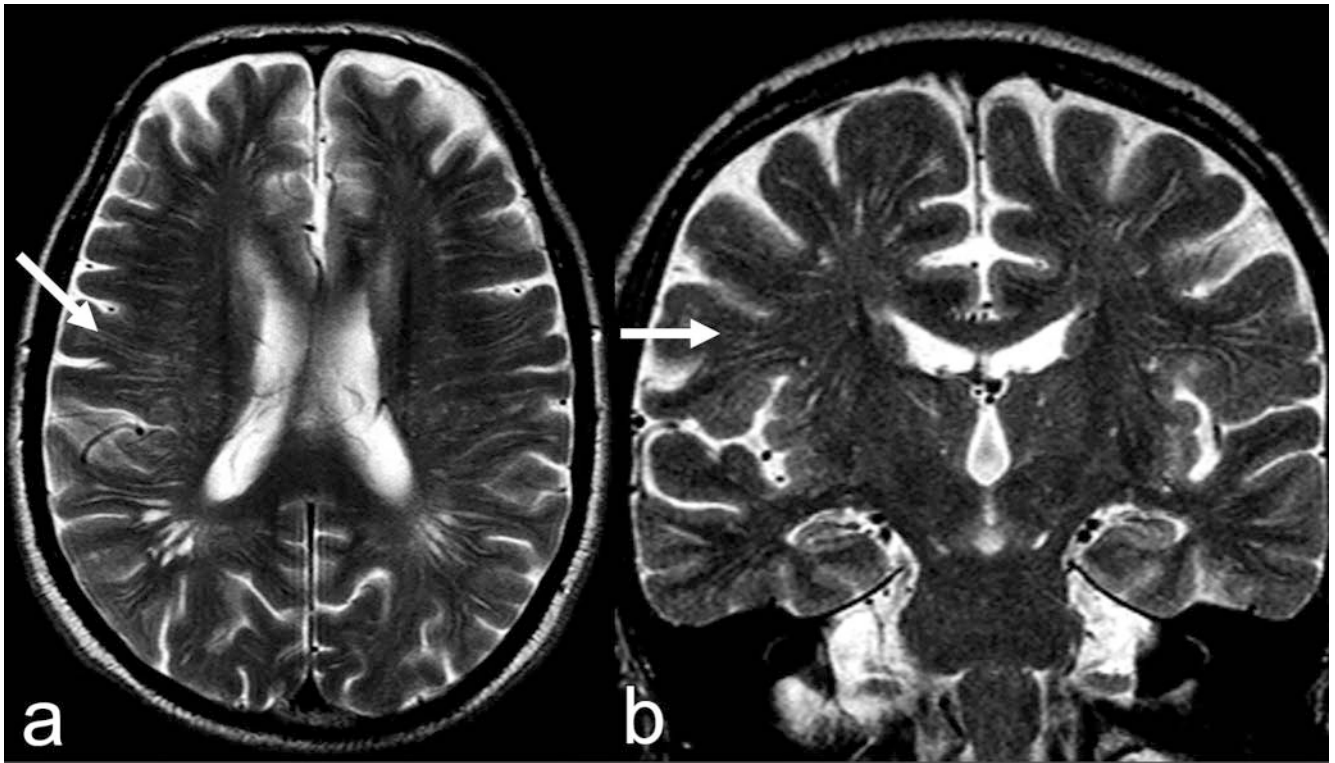
► **Fig. 2 a, b** Radial running perivascular spaces (PVS) with cerebrospinal fluid (CSF) isointense signal (**a, b**: arrows; T2 WI ax. and cor.).

4. Medullary white matter veins

Arterial and venous vascular systems run parallel in the white matter. Contrary to the arterial vascular supply, the veins penetrating the cortex are shorter and consequently the deep medullary veins draining to the medial center are longer, so that the venous watershed is closer to the brain surface [29].

5. Histological structure

a) Medullary white matter arteries

In the section near the origin, the terminal pial and medullary arteries are surrounded by pia mater and the subpial space to the brain parenchyma is delimited by the glia limitans [30]. Due to high cell density, this is very narrow at the level of the cortex and becomes subcortically widened [30, 31]. The lenticulostriate and thalamic perforators are surrounded by two leptomeningeal layers [28, 30].

b) Medullary white matter veins

The medullary veins are not enclosed by a pial layer; thus, the perivenous space communicates with the superficial subpial compartment [29].

c) Anterior outer edge of lateral ventricle ("Steiner's Wetterwinkel")

The white matter adjacent to the anterior horn and the cella media of the lateral ventricles is separated from the cerebrospinal fluid space by an only incompletely formed ependymal layer. This structure facilitates CSF diapedesis and causes age-related physiological appearance of hyperintense caps and strips on the T2 WI [6].
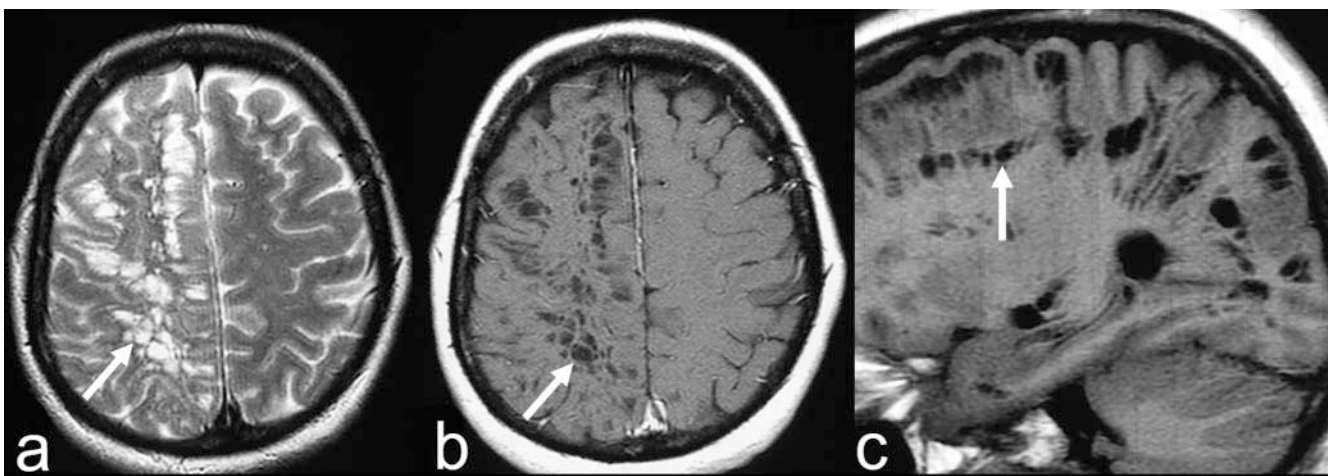
Para- and Perivascular Spaces (PVS)

Although the arterial subpial perivascular space is separated from the superficial subarachnoid space by the pia mater and filled with interstitial fluid [30], it appears CSF-isointense on the T2 WI, on FLAIR and on T1-weighted sequences (Virchow-Robin spaces, see ► **Fig. 2, 3**), and punctiform or elongated depending upon the section of the course of the penetrating arteries [1, 7–9]. These perivascular spaces can be cystically dilated (see ► **Fig. 4**) and in individual cases in mesencephalic position they can cause a disturbance of CSF circulation by constriction of the aqueduct [1, 9].

In addition to non-pathological congenital PVS size variations, increased dilation of these spaces in old age sometimes appears to be the result of impaired drainage of the interstitial fluid (glymphatic system) due to microangiopathy and represents possibly associated vascular induced impairment of cognition in the elderly [4, 23, 31–38]. The deposit of amyloid in the vessel walls near the cortex also have an amplifying effect. Expanded PVS can also occur in the context of metabolic diseases (see ► **Fig. 5**) [1, 15] and pathogen-induced inflammatory CNS diseases (see ► **Fig. 6**) [39]. The most common causes of cerebral white matter lesions are discussed below.
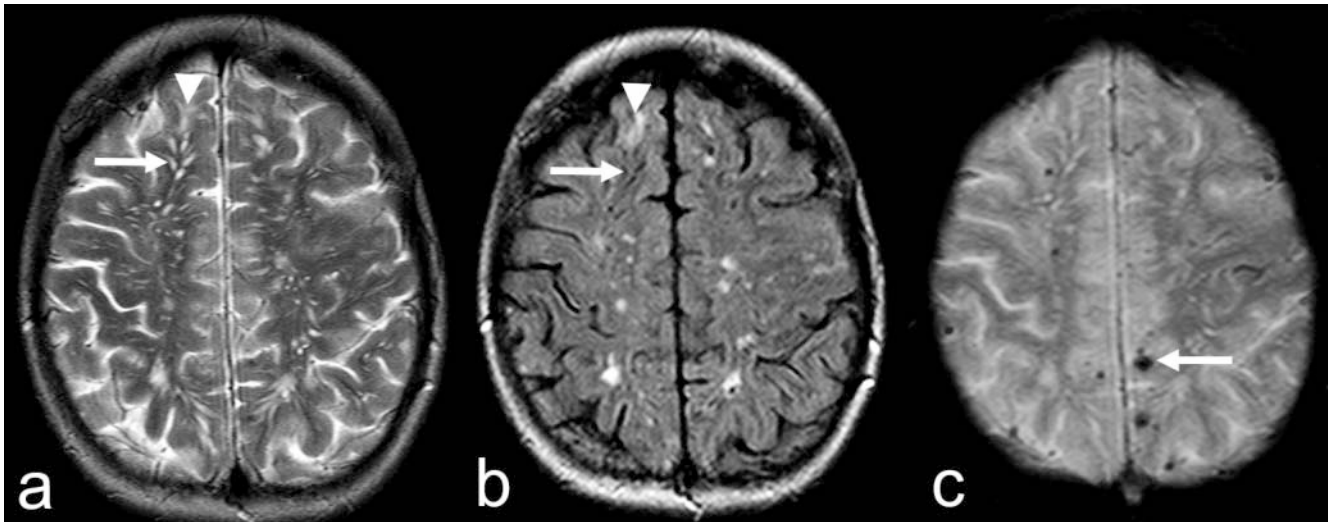
▶ **Fig. 3 a–c** Comparative signalling of anatomical and pathological structures. Dilated perivascular spaces (PVS) (**a**: T2 WI ax.; **b**: FLAIR ax., arrows) with sharply delineated cerebrospinal fluid (CSF) isointense signal; vascular gliosis with hyperintense signal changes (**a, b**: arrowhead). In addition, numerous subcortical hypointense lesions (microbleeds; **c**: arrowhead) in a patient with a brain-organic psychosyndrome due to cerebral amyloid angiopathy (CAA).

▶ **Fig. 4 a–c** Cystic dilated perivascular spaces (PVS) in a neurologically unremarkable patient (**a**: T2 WI ax.; **b, c**: T1 WI ax. and sag., arrow).

Microangiopathy (small vessel disease)

1. Vascularly-induced white matter signal changes (white matter changes; WMC)

PVS must be distinguished from vascularly-induced gliosis (see ▶ Fig. 3) which appears hyperintense on FLAIR sequences [1, 5, 7, 8]. Defective residuals after lacunar infarctions are CSF isointense and often have a narrow T2 hyperintense rim due to gliosis. They are oval or round-shaped with a longitudinal diameter ≤ 15 mm [3, 5, 7].

Vascular WMC are said to be caused by chronic hypoperfusion [40]. They typically occur bilaterally and symmetrically; 3 preferred regions are defined, whereby the perfusion areas in the terminal sections of the perforators play an important role: a) periven-

tricularly, b) in the deep white matter (centrum semiovale) and c) juxta- (sub-) cortically [10, 36]. The semiquantitative evaluation scale according to Fazekas et al. is often used [41, 42], whereby Grade 1 describes several punctiform lesions, Grade 2 partially confluent and Grade 3 extensive flat lesions (see ▶ **Fig. 7**).

As the volume of WMC increases, the risk of neurological functional deficits, infarcts, dementia and death increases [3, 4, 23, 32, 36, 43, 44]. While in age groups over 60 years WMC are typically found without a clinical correlate [35, 42], and some authors define age-associated WMC especially from the age of 75 years onward, there is no consistent information in the literature about the onset of these changes [43]. A higher incidence of WMC and possibly additional ovoid lesions in the border regions has also been described in patients with migraine with aura [45].
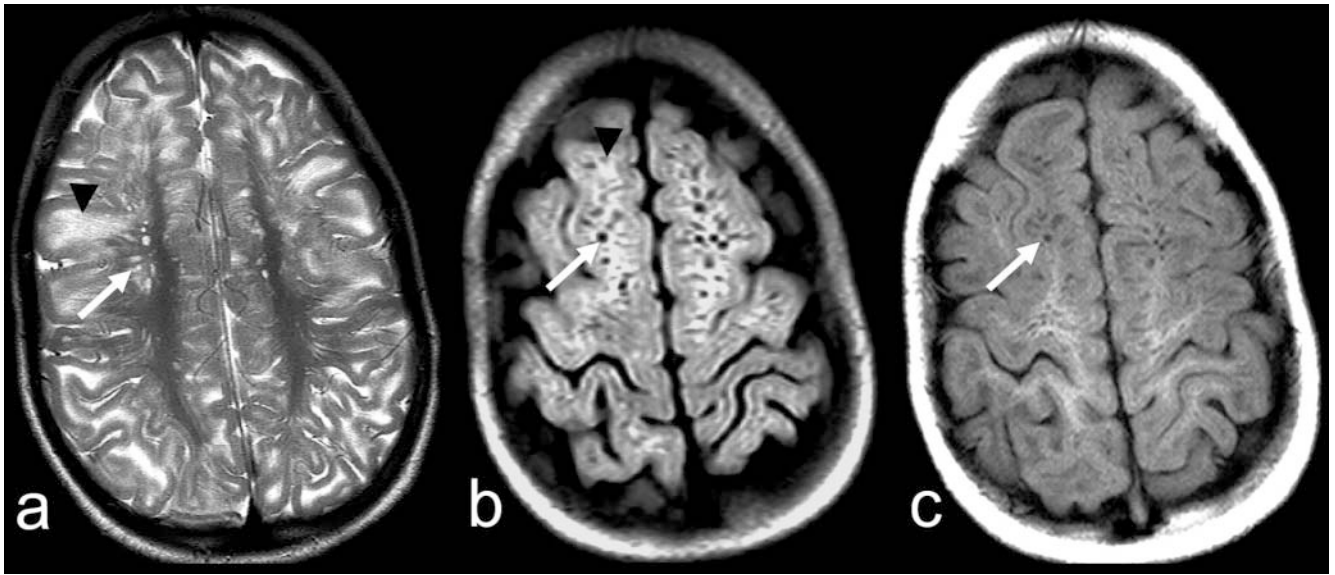
▶ **Fig. 5 a–c** Mucopolysaccharidosis. Enlarged perivascular spaces (PVS) (**a**: T2 WI ax.; **b**: FLAIR ax.; **c**: T1 WI ax., arrow) due to metabolite deposition ("Hurler holes") with accompanying glial reaction (**a, b**: arrowhead).
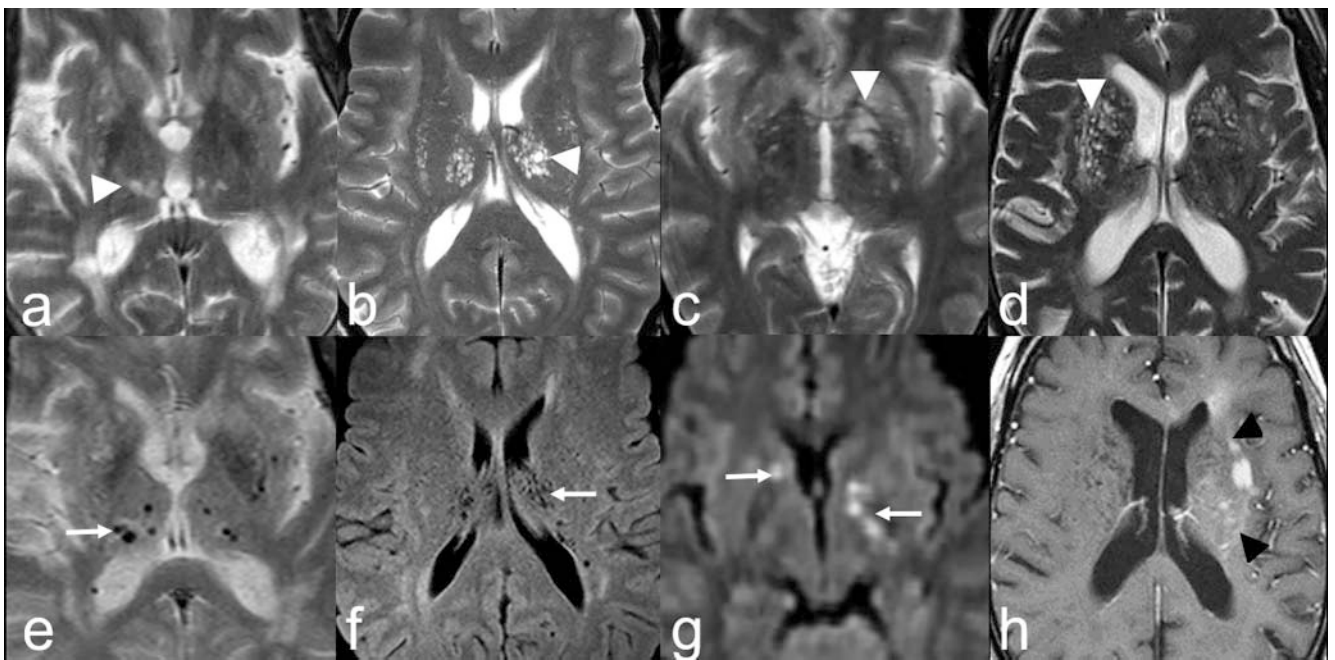
▶ **Fig. 6 a, e** Microangiopathic hyperintense lesions (**a**: T2 WI ax., arrowhead) with microbleeds (**e**: T2* WI ax., arrow); **b, f**: enlarged PVS in muco-polysaccharidosis ("Hurler holes"; **b**: T2 WI ax.; **f**: FLAIR ax.; arrowhead, arrow); **c, g**: Cryptococcosis; hyperintense lesions (**c**: T2 WI ax., arrowhead) in the course of lenticulostriate perforators with punctiform diffusion restrictions (gelatinous pseudocysts; **g**: DWI ax., b = 1000 s/mm², arrows); **d, h**: lymphoma with perivascular spread and enhancement in the left hemisphere (**h**: pc T1 WI ax., arrowheads), consecutive asymmetrical peri-vascular spaces (PVS) on T2 WI (**d**: arrowhead) in left-right comparison.

According to the etiopathogenetic classification of microan-giopathies defined by Pantoni [3], age-associated arteriosclero-sis with typical vascular risk factors (hypertension, diabetes mel-litus) dominates as Type 1 and sporadic and hereditary cerebral amyloid angiopathy (CAA) as Type 2 (see ▶ **Fig. 3**); together they comprise more than 90 % of microangiopathies. A common ima-ging characteristic of these etiologies is that white matter le-sions usually spare the corpus callosum [46–48]. Type 3 de-scribes other genetic microangiopathies (without CAA) such as CADASIL (Cerebral Autosomal Dominant Arteriopathy with Sub-
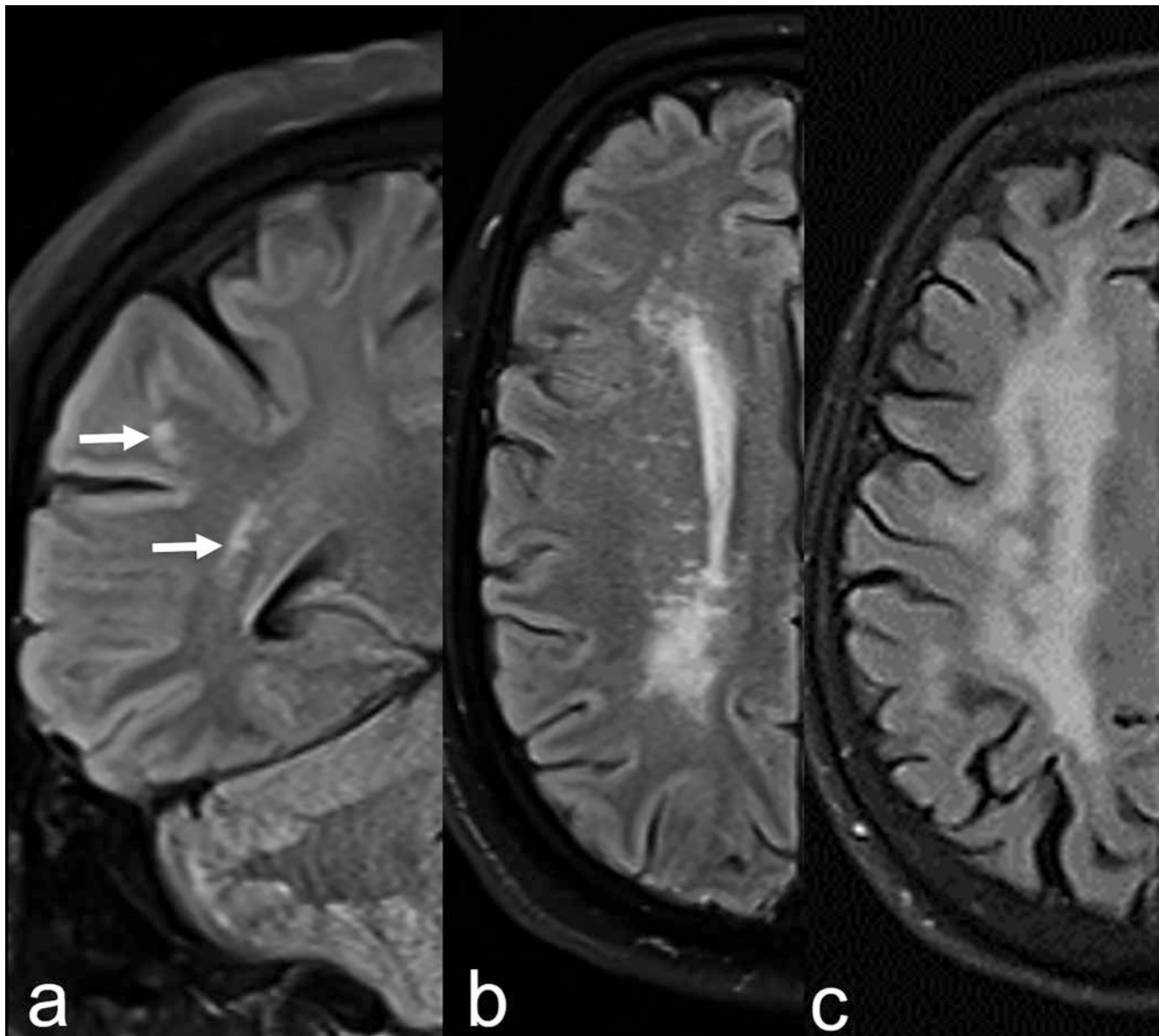
▶ **Fig. 7 a–c** Stages 1–3 according to Fazekas: single (**a**: FLAIR cor.; arrow), partially confluent and extended white matter changes (WMC) (**b, c**: FLAIR ax.).

cortical Infarcts and Leukoencephalopathy) (see ▶ **Fig. 8**) [40, 49], MELAS (Mitochondrial Encephalomyopathy with Lactic Acidosis and Stroke-like episodes) or Fabry disease [50, 51]. Type 4 includes inflammatory and immunologically mediated angiopathies; Type 5, venous collagenosis; and Type 6, other microangiopathies [52–54].
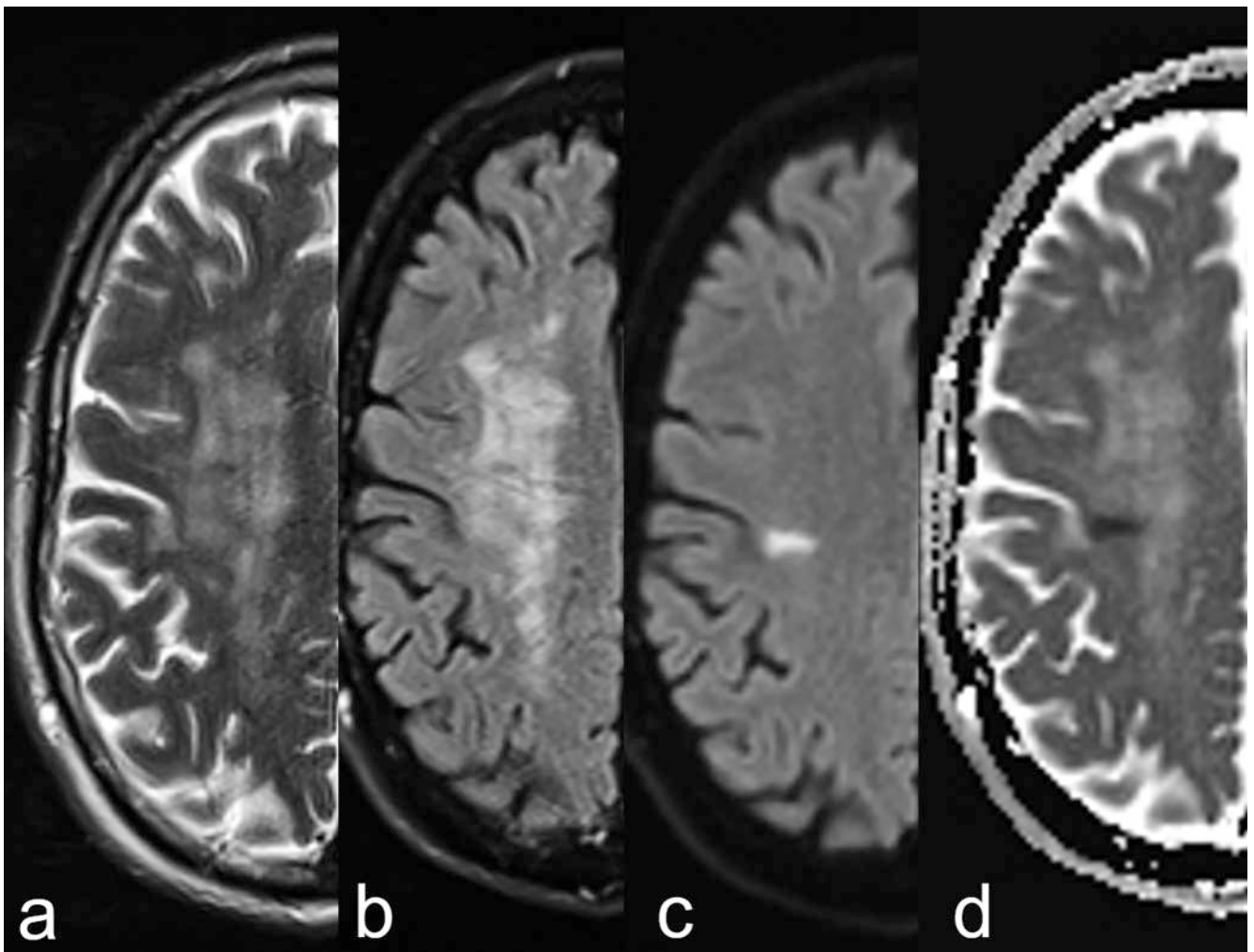
2. Lacunar infarcts

Follow-up examinations of cerebral microangiopathies have shown that a) incidental lacunes typically develop close to the edge of WMC, taking into account the course of the perforators [40]; b) the increase in WMC develops from periventricular to central subcortically, and c) WMC increases around an incidental

lacuna [40]. However, lacunes can also be caused by a macroangiopathy with atheromatous compromise of the perforator orifices, e.g. at the M1 segment of the middle cerebral artery, or by an embolism [3, 4, 33, 35, 55]. In the acute and subacute phase, DWI with evidence of a diffusion disorder due to circumscribed cytotoxic edema allows a reliable differentiation from pre-existing chronic WMC (see ▶ **Fig. 9**) [1, 5]. Macroangiopathy with corresponding upstream hemodynamically effective stenosis and possibly additional lesions in the border zone or terminal vascular bed is often present in the case of asymmetric WMC (see ▶ **Fig. 10**).

However, it is important to remember here that both autoimmune-associated inflammations such as multiple sclerosis (MS)
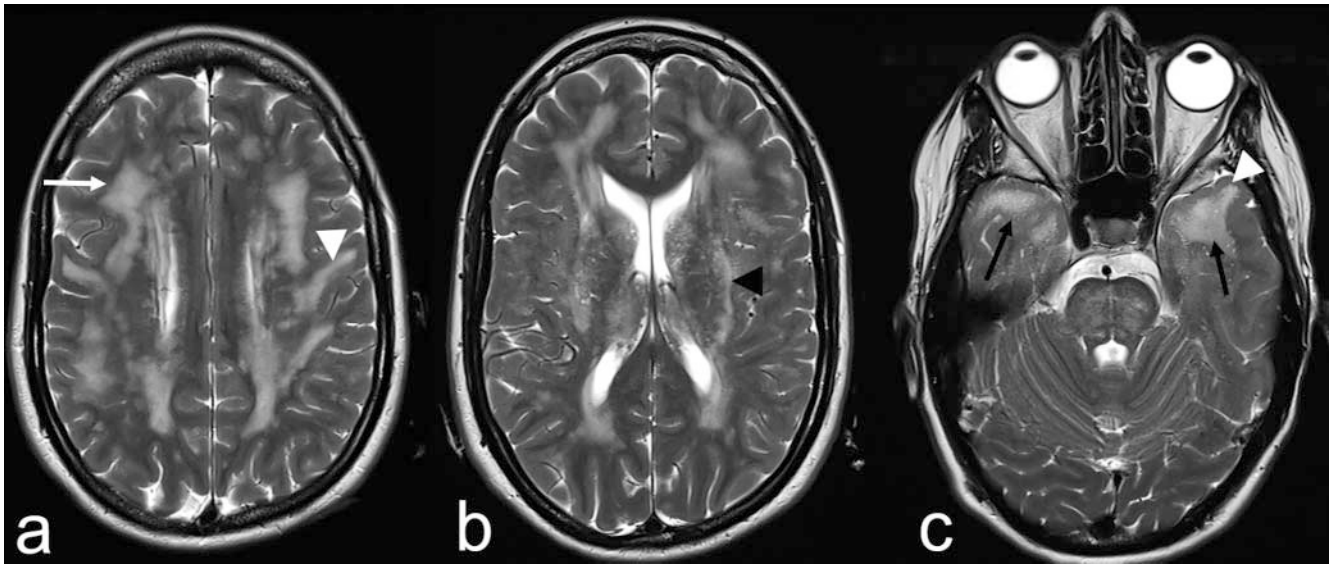
▶ **Fig. 8 a–c** Axial T2 WI in a 45 year old woman suffering from CADASIL showing partially confluent and nearly symmetrical hyperintense lesions in the deep white matter (**a**: arrow), in the external capsule (**b**: black arrowhead) and the anterior temporal pole (**c**: black arrow); involvement of the U-fibres (**a, c**: white arrowhead).

▶ **Fig. 9 a–d** Extended white matter changes (WMC) (**a, b**: T2 WI and FLAIR ax.) and additional acute lacunar infarct on the edge of the WMC (**c, d**: DWI ax; b = 1000 s/mm²; ADC-map).
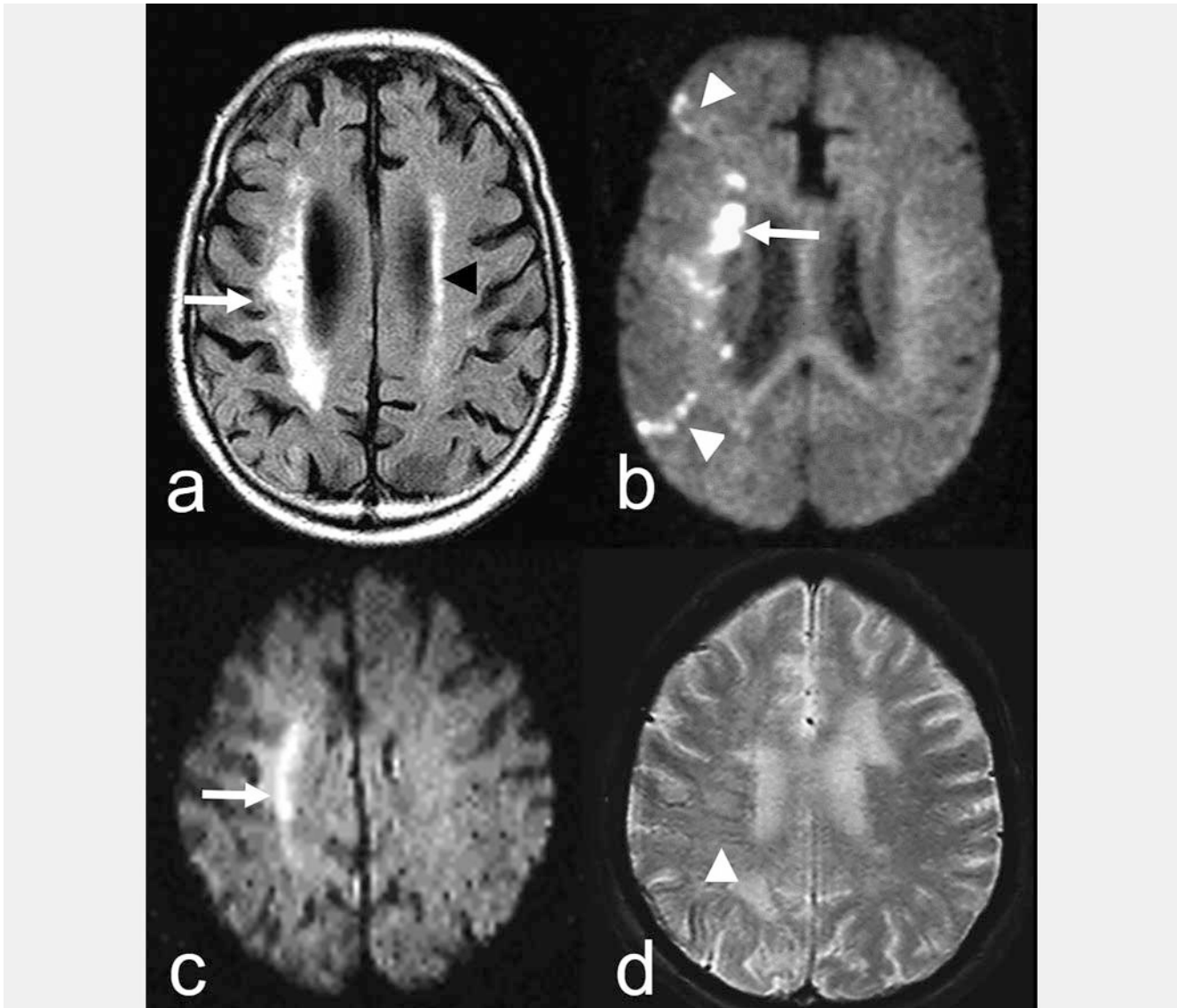
▶ **Fig. 10 a–d** Cytotoxic edema. Hemodynamically induced infarcts in the deep white matter (**b**: DWI; b = 1000 s/mm², arrow) and border zones (**b**: arrowhead) between the ACA, MCA and PCA territories right due to ipsilateral proximal ICA stenosis with asymmetrical white matter changes (WMC) (**a**: FLAIR ax., arrow, arrowhead); **c** (DWI ax.; b = 1000 s/mm²) and d (T2* WI ax.): hemodynamic infarct in the deep white matter right (**c**: arrow) and "dark vein sign" (**d**: arrowhead) due to increased oxygen extraction.

[12, 56–58] or NMOSD (Neuromyelitis Optica Spectrum Disorders) [59, 60] as well as pathogen-related infections can cause a diffusion restriction in the acute phase, although it is usually lesser compared to an acute cerebral infarction (see ▶ **Fig. 11**) [39]. In contrast to cytotoxic edema, vasogenic edema, particularly in blood-brain barrier disruption, typically shows an anatomically predetermined extension along fascicles and fiber structures (see ▶ **Fig. 12**) [2, 6].

3. Microbleeds (MB)

The detection of MB with blood-sensitive sequences such as T2*-weighted gradient echo (GRE) sequences or susceptibility-weighted imaging (SWI) with frequently punctiform signal can-

cellation as well as evaluation of their localization are essential for differential diagnostic assessment [46–48, 61]. MB in the basal ganglia, thalamus, pons or cerebellum are usually caused by hypertensive vasculopathy with lipohyalinosis of the perforators; signal reductions correspond to hemosiderin deposits in the degeneratively altered vessel walls [7, 48]. Intracerebral bleeding typically occurs here, especially in cases of arterial hypertension. Often there are also dilated PVS up to so-called status criblosus ("état criblé") and with sufficient high microscopic resolution the previously described "Charcot-Bouchard aneurysms" correspond to elongated and torqued perforators [8, 9, 46]. Differential diagnostically, cavernomas and parasitic/infectious diseases must be distinguished from MB.
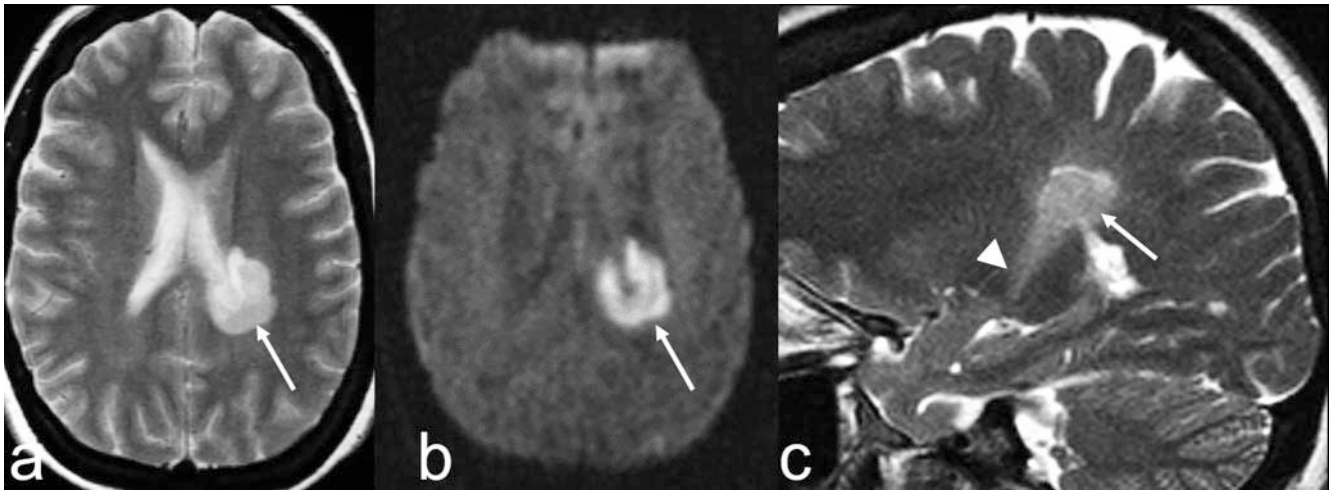
▶ **Fig. 11 a–c** Cytotoxic edema due to autoimmune-associated inflammation in a 34-year-old woman suffering from neuromyelitis optica spectrum disorders (NMOSD) with progressive hemiparesis re. within 3 hours. Axial T2 WI **a** disclose a polycyclic hyperintense lesion with broad contact to the left lateral ventricle (arrow); diffusion restriction (**b**: DWI; b = 1000 s/mm^2, arrow) and expansion along the corticospinal tract (**c**: T2 WI sag., arrow, arrowhead).
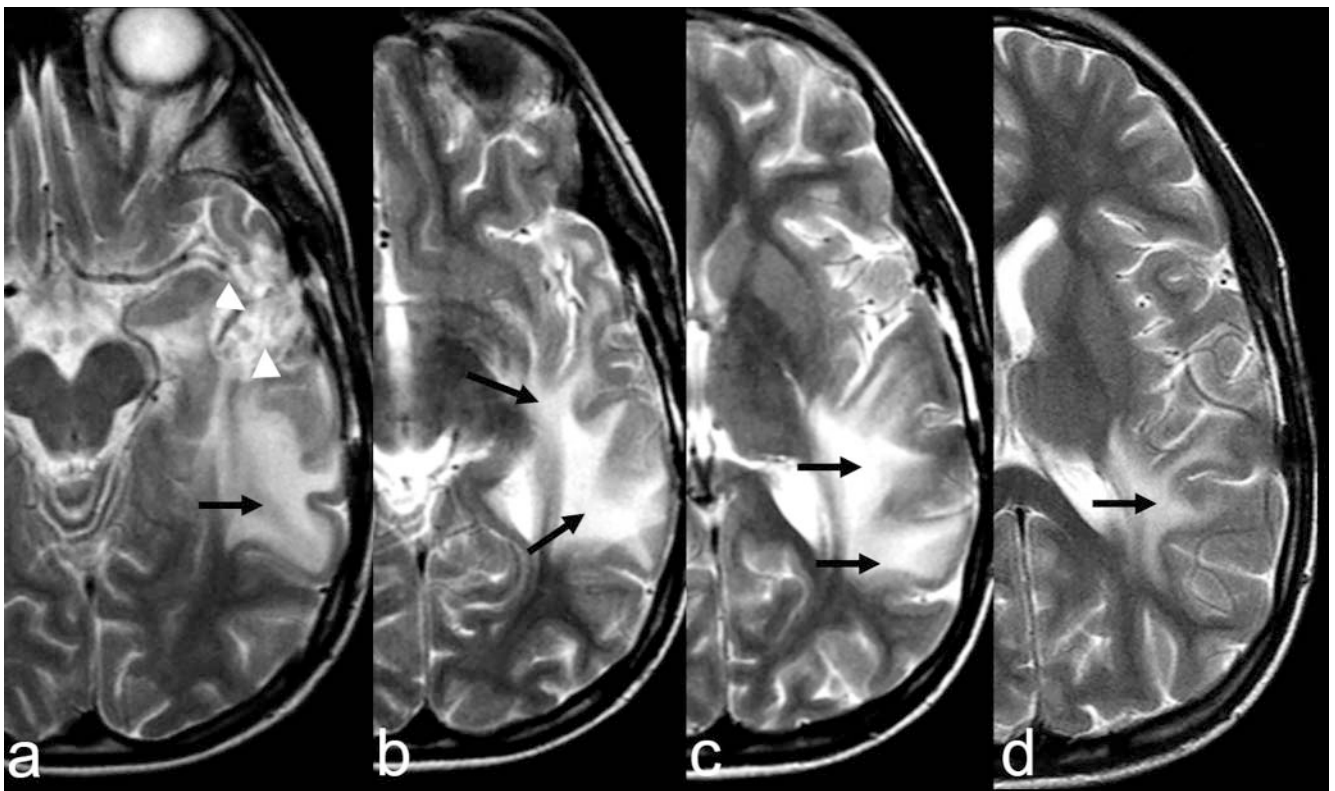
▶ **Fig. 12 a–d** "Finger-shaped" vasogenic edema (**a–d**: T2 WI ax., black arrows) corresponding to the course of the longitudinal inferior fascicle due to malignant glioma temporal left (**a**: arrowheads) with blood-brain barrier disruption.

Subcortical MB suggest CAA. In addition to microhemorrhages, the revised Boston criteria [47, 48] also include focal cortical superficial siderosis (see ▶ **Fig. 13**) [61]. In CAA, small cortical and subcortical arteries with a diameter < 500 μm, capillaries, and to a lesser extent veins, are affected by amyloid deposits in the vessel walls. In the course of the disease, the neocortex in front of the allocortical areas is affected, and there is a close correlation with Alzheimer's desease (AD) in parieto-occipital and temporal position (see ▶ **Fig. 13**) [23, 31, 62]. One variant is CAA-associated inflammation (CAA-RI), which histologically is
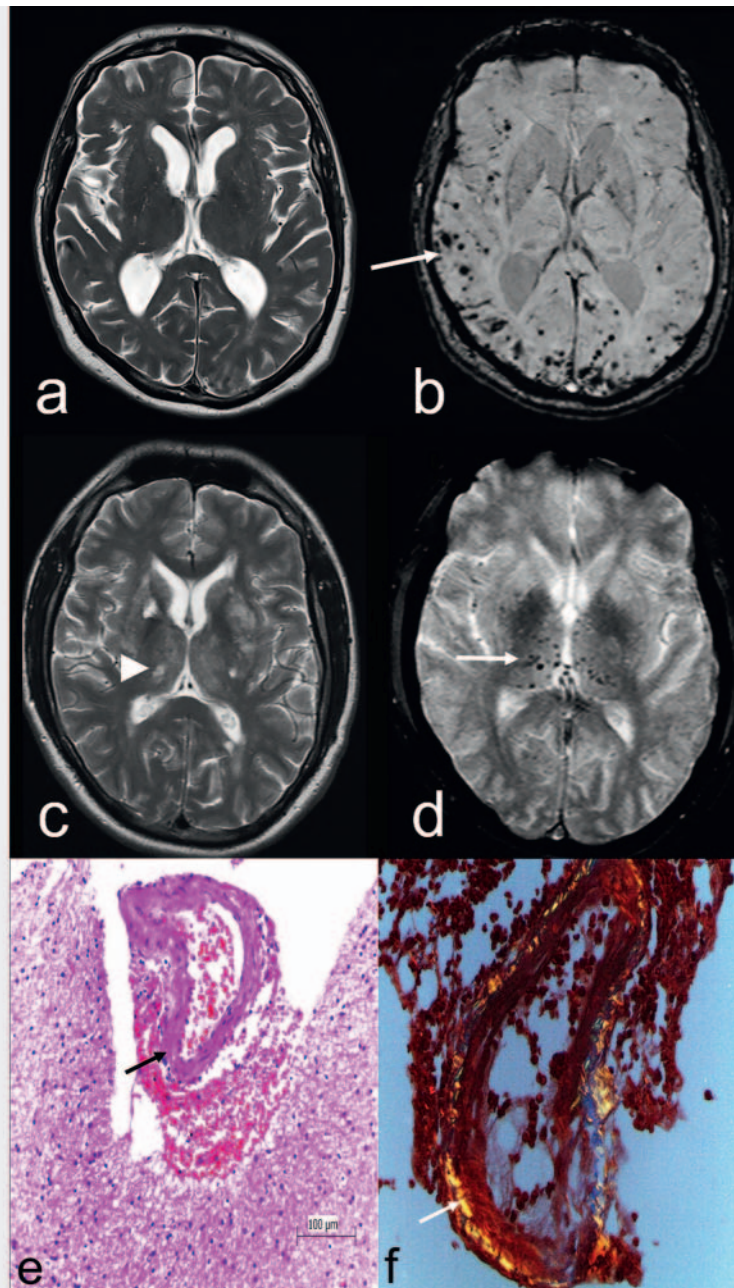
► **Fig. 13 a–d** Multiple microbleeds (MB) typically in the subcortical and cortical regions (**b**: SWI ax., arrow) in cerebral amyloid angiopathy (CAA) (**a**: T2 WI ax.); **c** (T2 WI ax.) and **d** (T2* WI ax.): MB especially in the basal ganglia and thalamus (**d**: arrow) due to lipohyalinosis of the basal perforators with vascular gliosis and lacunar infarcts (**c**: arrowhead). **e, f**: Histological specimen in atypically located intracerebral haemorrhage due to cerebral amyloid angiopathy (CAA): amyloid in the artery wall (**e**: arrow; HE staining) with birefringence in polarized light and typical "apple green" colour (**f**: arrow).

perivasculitis and associated with extensive, sometimes space-occupying lesions in the white matter (see ► **Fig. 14**) [63, 64]. The lesion type is similar to that described in therapy studies with monoclonal antibodies against amyloid beta 42 (Aβ-42) in patients with AD [65]. The authors distinguish a hemorrhagic and an encephalitic variant (Amyloid-Related Imaging Abnormalities; ARIA-H, ARIA-E). For the sake of clarity, amyloid-β related angiitis (ABRA) and its differentiation from primary CNS angiitis (PCNSA) will not be discussed in detail; the latter exhibits no amyloid deposits [54, 63, 64]. If MB are subcortical and/or in deep white matter adjacent to various old (lacunar) infarcts and additional WMC, differential diagnosis should consider vasculitis of possibly only the small vessels (Pantoni Type 4) [3, 52]. In this context, reference is also made to the revised Chapel Hill 2012 criteria on systemic vasculitis [53].
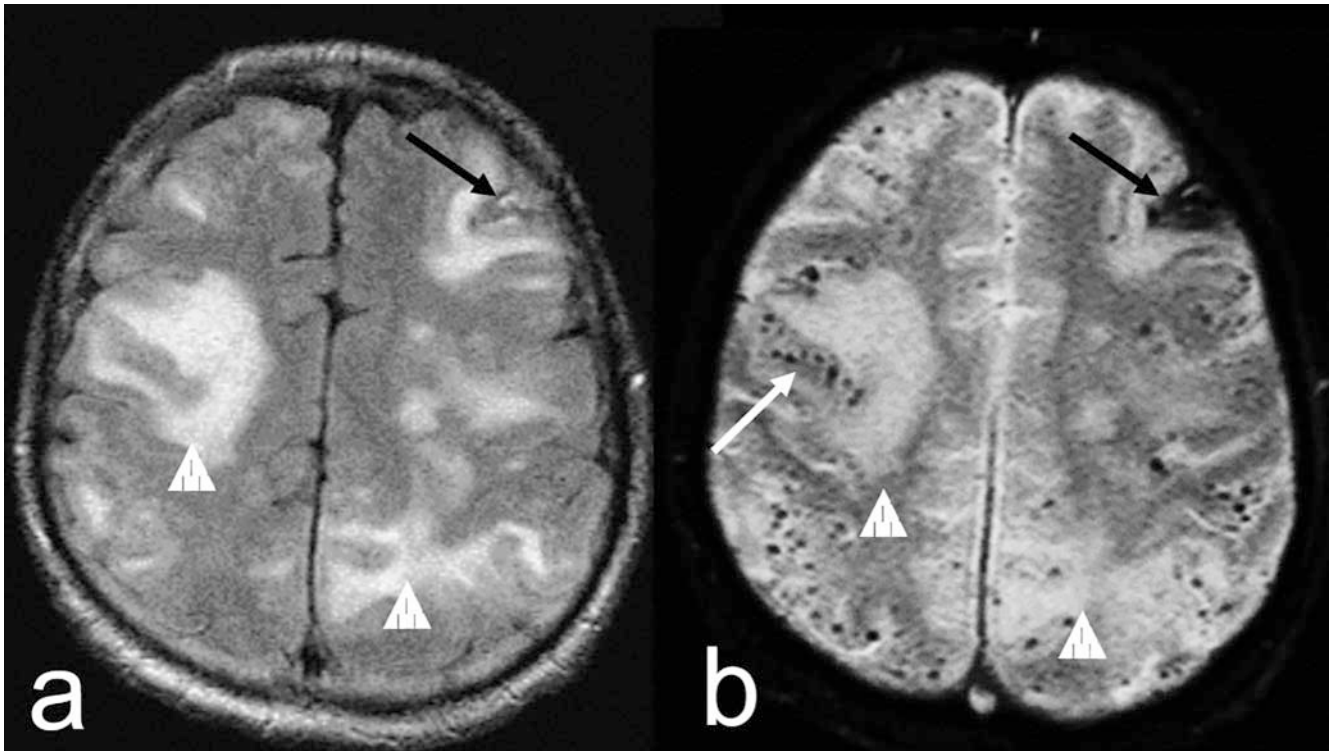
▶ **Fig. 14 a, b** Inflammatory variant of cerebral amyloid angiopathy (CAA – RI): extensive hyperintense lesions associated with swelling (**a**: FLAIR ax.; **b**: T2* WI ax., arrowhead) with pearl-like multiple cortical and subcortical microbleeds (MB) (**b**: arrow) and residual atypical frontal left-sided haemorrhage (**a, b**: black arrow) in a 73 year old man suffering from progressive dementia.

## Angiocentric Propagation Pattern

Vascular-associated diseases as well as inflammatory and neoplastic processes may exhibit an angiocentric lesion pattern on T2 WI due to the anatomically predetermined propagation along the PVS, which is illustrated by taking into account the T1 WI after contrast application (pc T1 WI) [39, 66–69]. In addition to sarcoidosis (see ▶ **Fig. 15**) [67, 68], in particular fungal infections [39], primary CNS lymphoma (PCNSL) as well as related diseases (e. g. lymphomatoid granulomatosis) [70] show a streaky or punctiform enhancement, with possibly continuous Gadolinium enhancement of the perivascular leptomeningeal structures along the course of the perforators with differently pronounced perifocal edematous (T2-hyperintense) reaction and possible circumscript diffusion restriction due to inflammation, high cell density or a resulting infarction.

## Perivascular Inflammatory Lesions in Multiple Sclerosis (MS)

Multiple sclerosis (MS) is the most common demyelinating disease. The 2017 revisions of the MRI criteria for diagnosis define four characteristic regions for dissemination in space (DIS): a) juxta-/cortical, b) periventricular, c) infratentorial and d) spinal [12, 57, 58, 71]. Spatial dissemination requires at least one T2 hyperintense lesion in at least two regions, whereby a longitudinal extension of ≥ 3 mm is required e. g. periventricularly for lesions that often run perpendicularly to the ventricular wall (Dawson's finger; see ▶ **Fig. 16, 17**) [57, 58]. Correlating with the histological description, the central vein in the plaques can be delineated at higher field strengths on SWI [12]. The simultaneous presence of a contrast enhancing lesion and a non-enhancing lesion, or a new lesion that occurs in the course of the disease, are criteria for dissemination in time (DIT) [57]. In contrast to atherosclerotic microangiopathy, U-fibers are also affected in juxtacortical MS lesions [57, 72]. The corpus callosum lesions previously considered typical for MS do not belong to the four spatial categories defined above, and despite their ventriculotopic location, differential diagnosis includes vasculitis (see ▶ **Fig. 18**) [11, 52, 54, 68]. Cotton wool-like cloudy hyperintense lesions on T2 WI located centrally in the corpus callosum are described in Susac Syndrome [73].

In the case of acute demyelinating encephalomyelitis (ADEM), numerous monomorphic lesions, often with blurred boundaries, are clearly visible subcortically and in the basal ganglia with marginal contrast enhancement open towards the cortex ("open ring") [11, 74]. A marked perivenous orientation of white matter lesions is also described in Behçet's disease and in ANCA (anti-neutrophil cytoplasmic antibodies) associated vasculitis of the small vessels (e. g. microscopic polyangiitis) corresponding to its manifestation in capillaries and veins [75–77]. Regarding the ex-
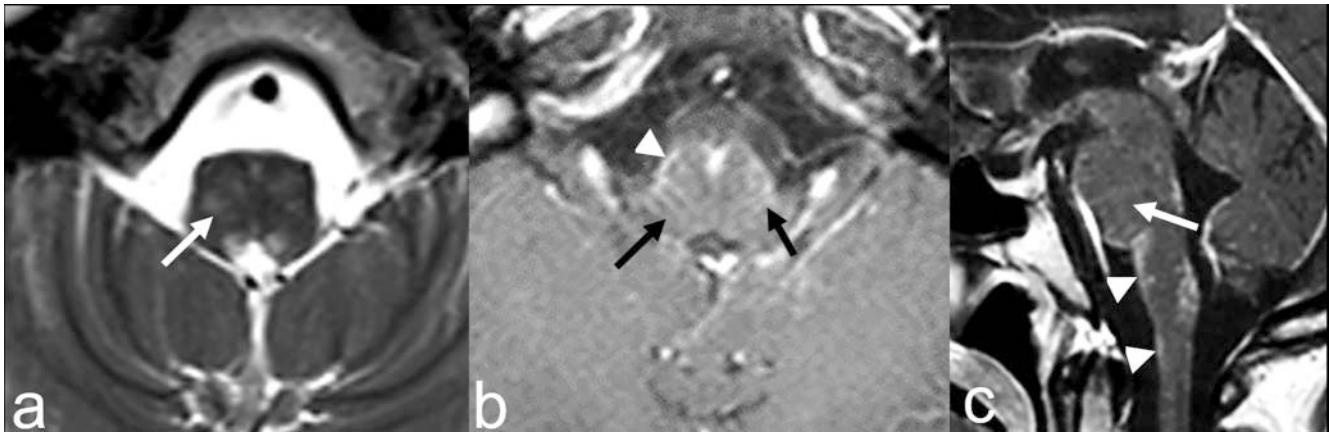
▶ **Fig. 15 a–c** Angiocentric lesion pattern in sarcoidosis. Symmetrical blurred lesions in the pons (**a**: T2 WI ax., arrow) with enhancement (**b, c**: pc T1 WI ax. and sag.; arrows) in the course of the perforators; note also superficial pial enhancement (**b, c**: arrowheads).
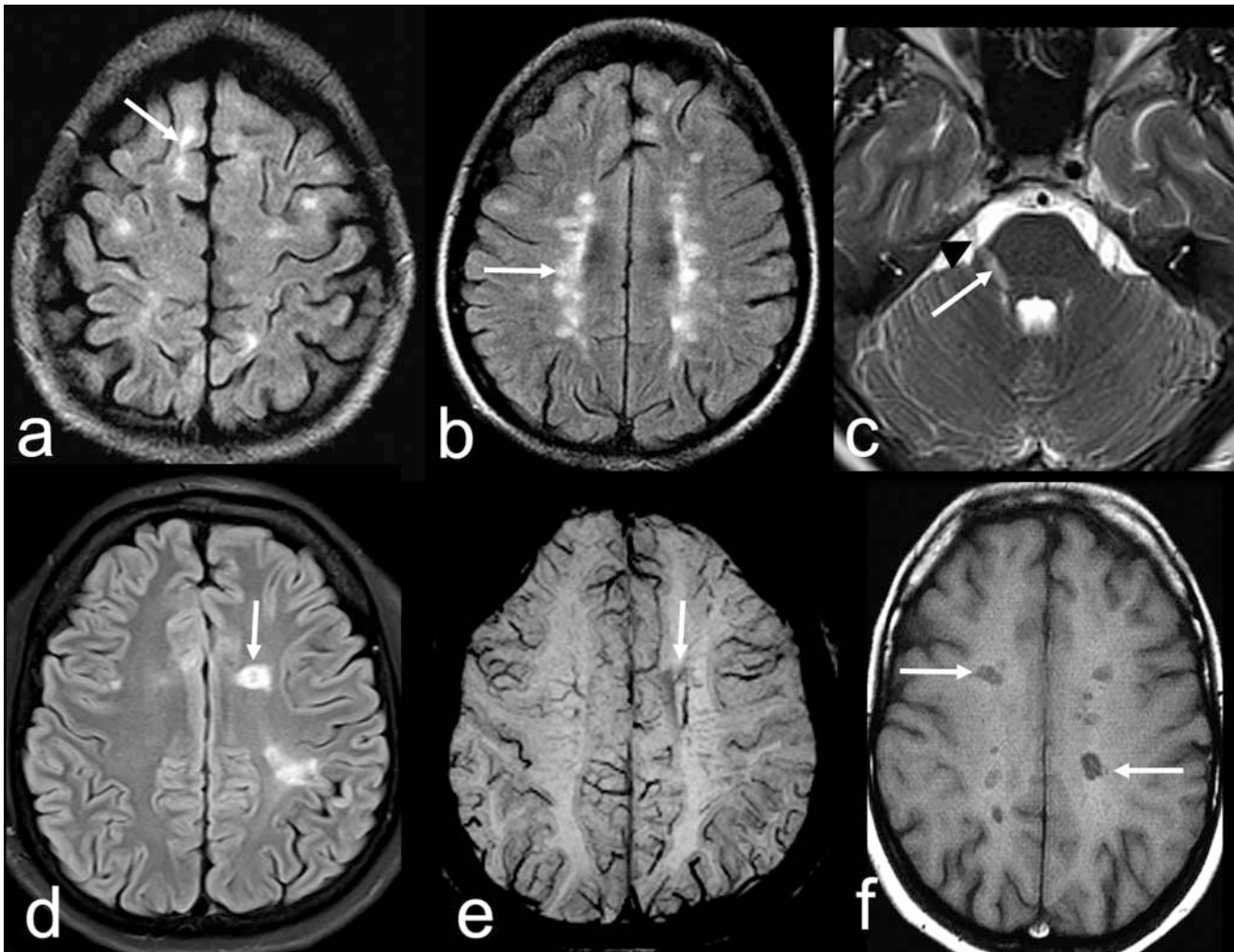
▶ **Fig. 16 a–f** Multiple sclerosis (MS): Juxtacortical, periventricular (**a, b**: FLAIR ax., arrows) and infratentorial lesions (**c**: T2 WI ax.; arrow: trigeminal nerve nucleus; arrowhead: trigeminal nerve); **d** (FLAIR ax.) and **e** (SWI ax.): periventricular plaque (**d**: arrow) with central vein (**e**: arrow); **f** (T1 WI ax.): "black holes" (arrows).
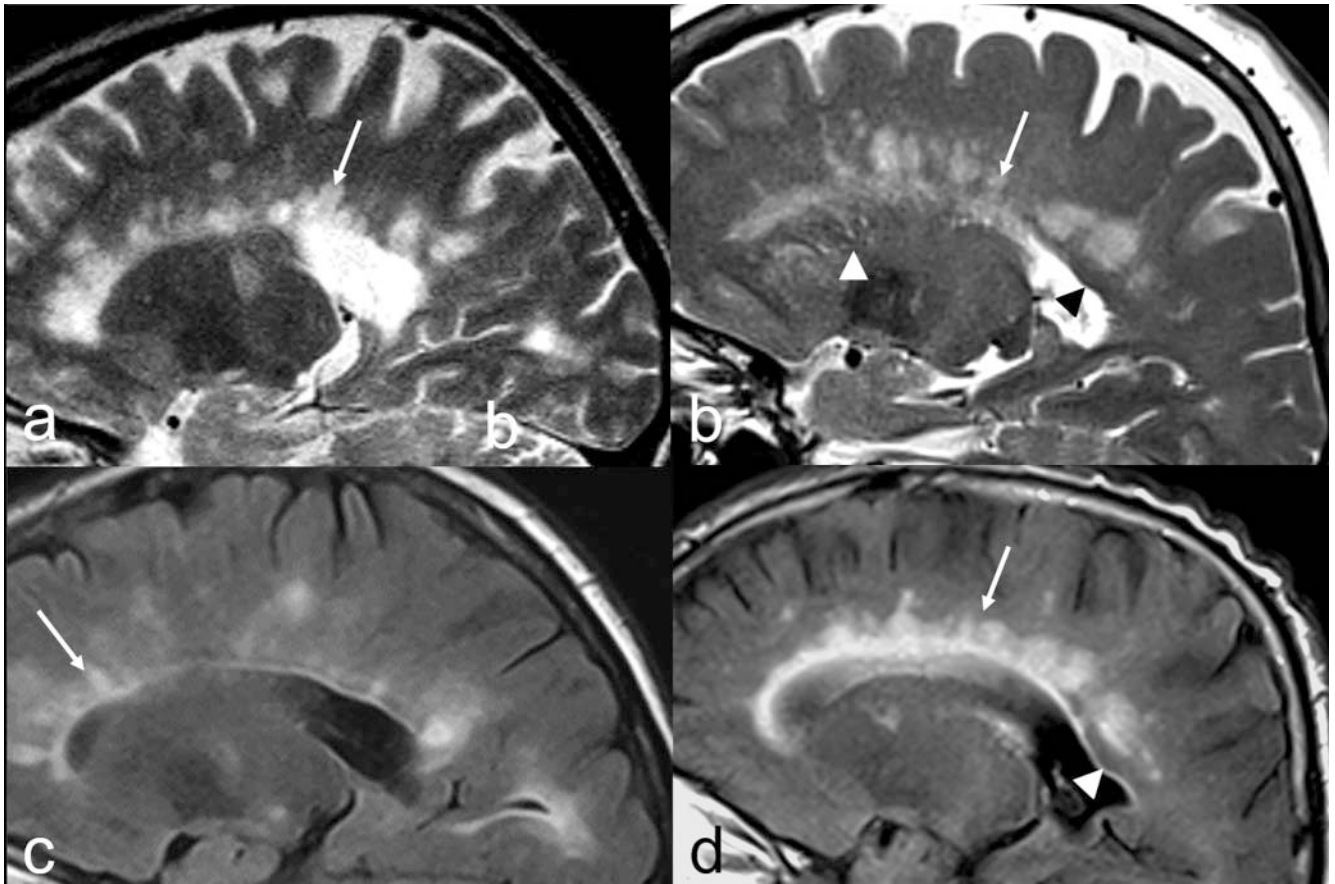
▶ **Fig. 17** **a, c** Perivenous radially oriented hyperintense lesions in multiple sclerosis (MS) (Dawson's finger; **a**: T2 WI sag.; **c**: FLAIR sag., arrows); **b, d**: angiocentric arterially oriented hyperintense lesions due to microangiopathy (**b**: T2 WI ax.; **d**: FLAIR ax., arrows) with dilated PVS (**b**: white arrowhead); note partially spared thin strip of periventricular myelin at the level of the ventricular trigonum (**b**: black arrowhead; **d**: white arrowhead).

tensive differential diagnosis of MS and atypical course variants, reference is made to the further special literature [68, 75].

Extensively Spread Lesions

The differential diagnosis of larger extended, often homogeneous white matter lesions includes metabolic (e. g. leukodystrophies, vitamin B12 deficiency, others) [22, 23, 78], inflammatory (e. g. HIV encephalopathy, progressive multifocal leukoencephalopathy; PML) [79–82], toxic (e. g. heroin-induced spongiform leukoencephalopathy) as well as radiogenic causes [18, 19]. Assessment of U-fiber involvement in addition to symmetry is necessary for a closer differential-diagnostic classification. PML emanating from the oligodendrocytes can be the overture to previously unrecognized immunosuppression due to HIV disease [39, 82]. Typical asymmetrical white matter changes are not space-occupying; they expand extensively along fiber tracts and involve the U-fibers (see ▶ **Fig. 19**) [80, 83]. T1 WI show a signal reduction and, depending on the immune status or the presence of an immune reconstitution inflammatory syndrome (IRIS), contrast accumulation and diffusion restriction may be present at the edges. In the case of therapy-related compromised immune

system (e. g. natalizumab), a punctiform perivascularly oriented enhancement can occur in the vicinity of hypointense lesions on pc T1 WI ("milky way") [83, 84]. In contrast, HIV-induced progressive diffuse leukoencephalopathy (PDL) typically spares the U-fibers (see ▶ **Fig. 19e**), is rather symmetrical and non- to slightly-hypointense on T1 WI. HIV encephalitis as an acute variant also affects the gray matter [39, 79].

Of the large heterogeneous group of leukodystrophies, metachromatic leukodystrophy (MLD) and adrenoleukodystrophy (ALD) deserve special mention, since both can also manifest clinically in advanced age [13, 22, 68]. Symmetrical, homogeneous changes in the white matter that leave out the U-fibers are apparent in the adult variant of MLD, which occurs in approx. 15 % of cases and exhibits clinically slowly progressive psychiatric symptoms (see ▶ **Fig. 19**). ALD preferentially affects the parietooccipital white matter, shows marginal contrast enhancement depending on the stage of the disease and spreads into the descending fiber tracts [22]. A disorder related to vanishing white matter diseases (VWMD) can occur at any age. Mitochondriopathies such as MELAS or Kearns-Sayre syndrome (KSS) often also exhibit cortical involvement [50].
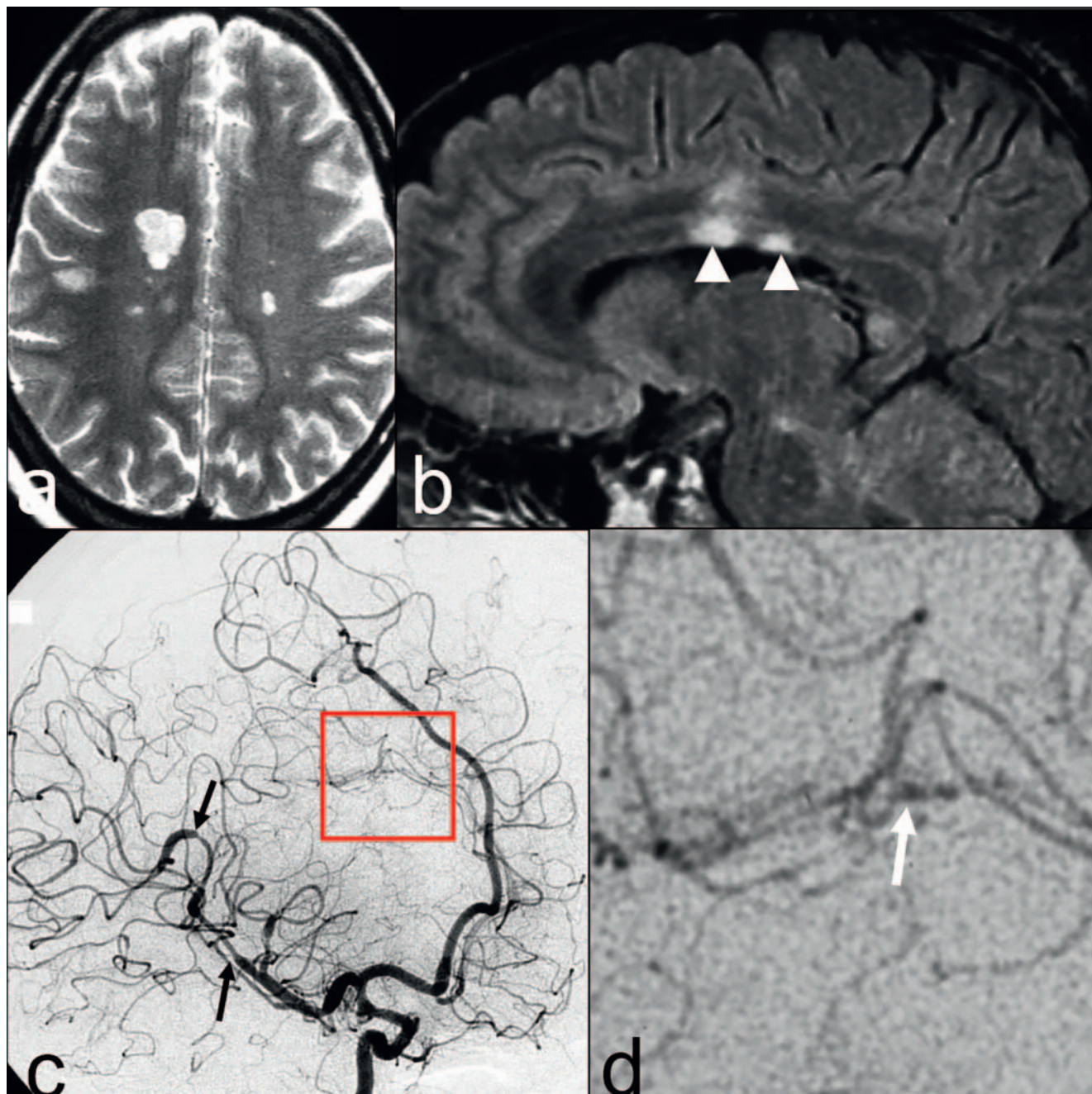
▶ **Fig. 18 a–d** Panarteritis nodosa. Hyperintense white matter lesions (**a**: T2 WI ax.) and involvement of the corpus callosum (**b**: FLAIR sag., arrowhead) due to vasculitis. Digital subtraction angiography (DSA) showing multiple vascular narrowings (**c**, arrows) and string of beads in the course of the pericallosal artery (**d**: arrow).

It is important to note that advanced chronic vascular and inflammatory etiologies may also exhibit extensive and largely symmetrical lesion patterns in the final stage [2].

Cell or System/Fiber Tract-associated Lesions

As an example from the group of neurodegenerative diseases, Waller's degeneration in amyotrophic lateral sclerosis (ALS) with variable involvement of the 1st and 2nd motor neuron is described here [85]. This results in a symmetrical signal increase on T2 WI in the course of the corticospinal tract starting directly below the primary motor cortex (see ▶ **Fig. 20**). The ALS dementia complex preferentially dicloses frontotemporal atrophy corresponding to a Tau protein negative, TDP-43 positive (TAR-DNA binding protein) frontotemporal dementia [23, 86]. Waller's degeneration of the corticospinal tracts can also occur after damage to the 1st motor neuron due to other causes, e. g. after (sub-) cortical infarcts [85].
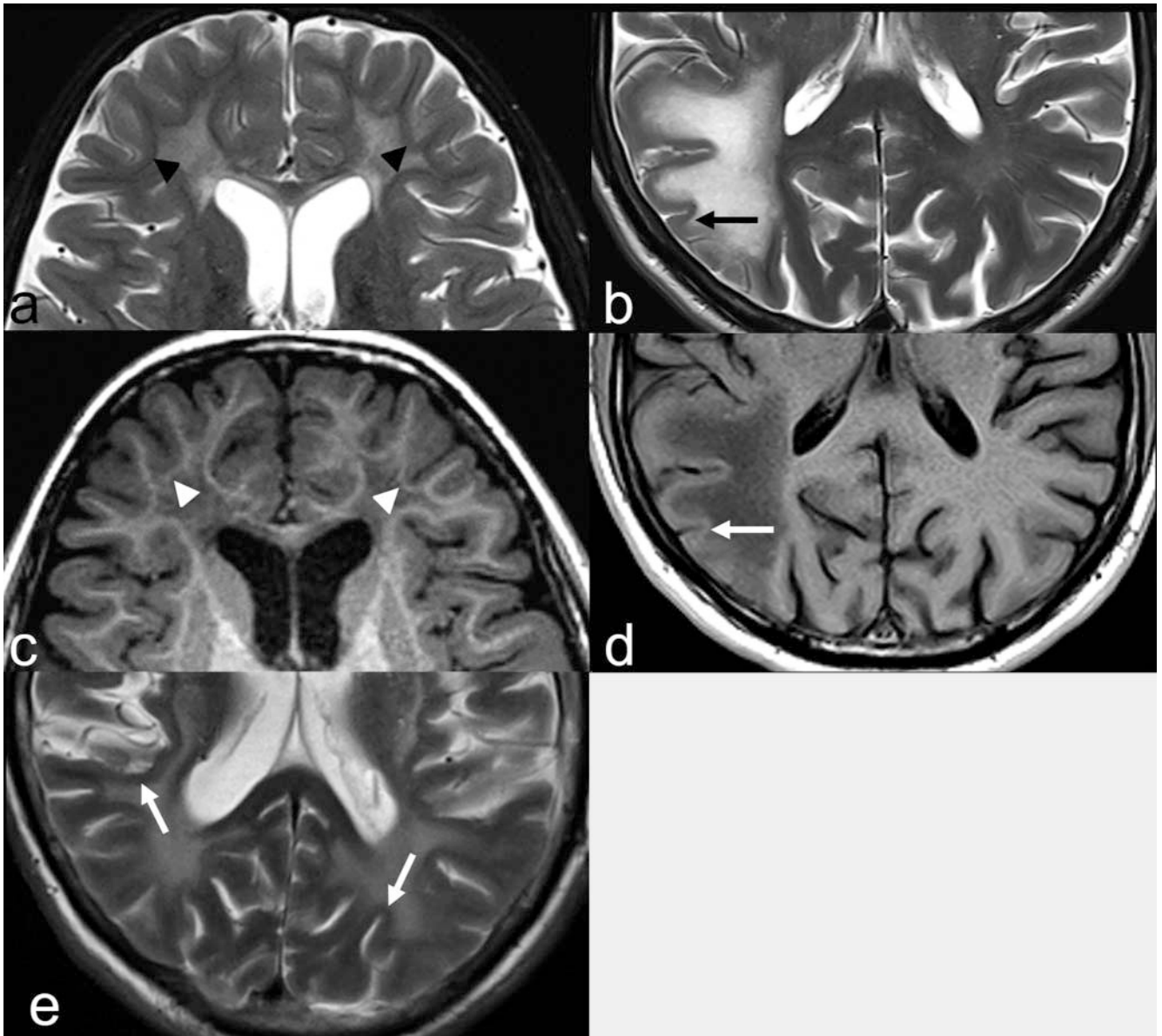
▶ Fig. 19 a–d U-fibres. a, c: Sparing of the U-fibres in metachromatic leukodystrophy (MLD) (a: T2 WI ax.; c: T1 WI ax., arrowheads); b, d: Involvement of the U-fibres in progressive multifocal leukoencephalopathy (PML) (b: T2 WI ax.; d: T1 WI ax., arrows). e: Sparing of the U-fibres in progressive diffuse leukoencephalopathy (PDL) due to HIV disease (T2 WI ax., arrows).

Checklist for Image Analysis and Diagnostic Algorithms

▶ Table 2 and ▶ Fig. 21 summarize various imaging findings and corresponding differential diagnostic aspects. The age of the patient, the progression of the disease and the clinical and neurological findings as well as previous illnesses and laboratory parameters must be taken into account.

Conclusion

Comparative image analysis of different identically angulated MRI sequences including DWI and T2* WI or SWI is a prerequisite for the reliable differential diagnostic assessment of white matter lesions. Characteristic lesion patterns can be identified, taking into account the architecture and vascular supply of the white matter. The etiology of white matter lesions includes vascular, inflammatory, metabolic and neoplastic processes. Vascular pathologies are in the foreground, especially in the elderly; age-associated arteriosclerosis with typical risk factors and CAA account for over 90 % of microangiopathies. Physiological changes such as dilated
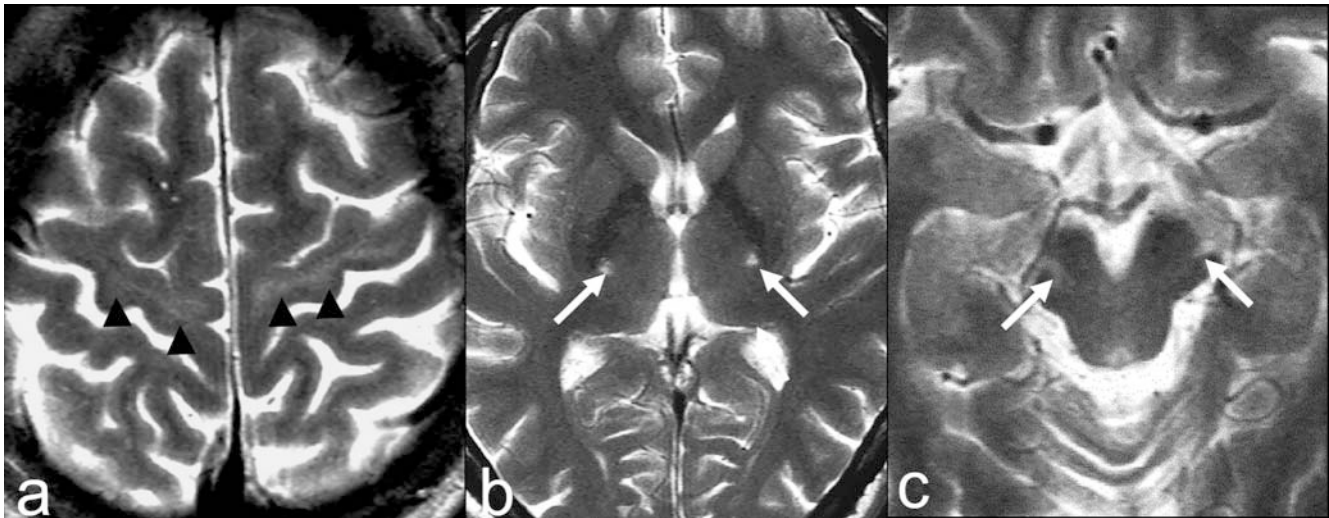
▶ **Fig. 20 a–c** T2WI showing symmetric system associated hyperintense signal changes in the course of the corticospinal tract: in the subcortical region of the precentral gyrus (**a**: arrow heads), in the internal capsule (**b**: arrows) and in the cerebral peduncle (**c**: arrows) due to amyotrophic lateral sclerosis (ALS).
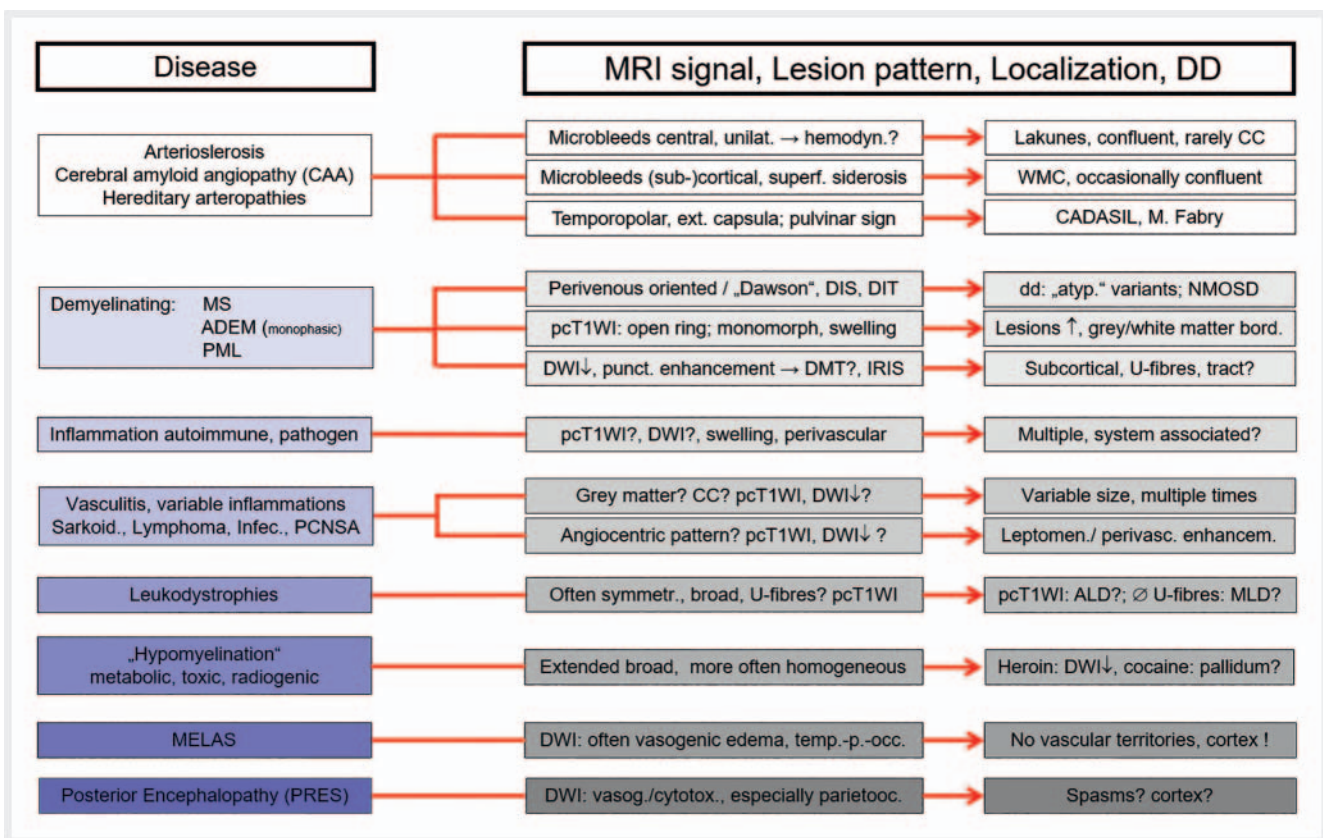
▶ **Fig. 21** White matter lesions in adults: hints for the differential diagnosis. ADEM: Acute demyelinating encephalomyelitis; ALD: Adrenoleukodystrophy; CAA: Cerebral amyloid angiopathy; CADASIL: Cerebral autosomal dominant arteriopathy with subcortical infarcts and leukoencephalopathy; CC: Corpus callosum; DIS: Dissemination in space; DIT: Dissemination in time; DWI: Diffusion weighted imaging; IRIS: Immune reconstitution inflammatory syndrome; MELAS: Mitochondrial encephalomyopathy with lactic acidosis and stroke-like episodes; MLD: Metachromatic leukodystrophy; MS: Multiple sclerosis; NMOSD: Neuromyelitis optica spectrum disorders; PCNSA: Primary central nervous system angiitis; PML: Progressive multifocal leukoencephalopathy; WMC: White matter changes.

▶ **Table 2** Checklist for image analysis and differential diagnostic hints.

lesion		pattern	diagnostically indicative of
white matter changes (WMC)	manifestation	(e. g. Fazekas I–III) "age-associated"?	microangiopathic fibrohyalinosis
	location	centrum semiovale, periventricular	
		temporopolar, external capsule	CADASIL
		U-fibers involved	PML
		lateral difference, border regions	upstream stenosis
		symmetrical	HIV, metabolic, genetic
	lacunes	quantity, position	DD: PVS?
microbleeds (MB)	location	basal ganglia, thalamus, pons, cerebellum	microangiopathic fibrohyalinosis
		subcortical, accompanying superficial siderosis and atypically localized microbleeds	CAA
diffusion restrictions	lacunar	oval, round; ≤ 15 mm diameter	lacunar infarction due to microangiopathy
		additional cortical infarctions	vasculitis
		in vascular border zones / terminal vascular territories	hemodynamic infarct, macroangiopathy
		dark vein sign	hemodynamic infarcts, upstream stenosis
	inflammatory	individual lesions	inflammatory cell infiltration in MS, ADEM, other
		perivenous, centrum semiovale	MS
		(immunosuppressive) medication, broad, > 15mm; peripheral	opportunistic infection
		cortex involvement	MS
	metabolic	metabolic stroke	metabolic disease, mitochondriopathy
		diffuse	intramyelinary edema
		corpus callosum involvement	anti-epileptic therapy (reduction)
perivascular spaces (PVS)	location	basal ganglia, anterior commissure, centrum semiovale	
	manifestation	cystic expansion, lateral difference	
	signal abnormalities	signal alteration on FLAIR, DWI, enhancement	cryptococcus, granulomatous inflammation, lymphoma
contrast enhancement	manifestation	broad, angiocentric pattern	sarcoidosis, lymphoma, meningeosis
	pattern	PVS, leptomeningeal involvement, vessel walls	sarcoidosis, infection (fungal), vasculitis

ADEM: Acute Demyelinating Encephalomyelitis; CAA: Cerebral Amyloid Angiopathy; CADASIL: Cerebral Autosomal Dominant Arteriopathy with Subcortical Infarcts and Leukoencephalopathy; DD: Differential diagnosis; DWI: Diffusion-Weighted Imaging; FLAIR: Fluid Attenuated Inversion Recovery; HIV: Human Immunodeficiency Virus; MS: Multiple Sclerosis; PML: Progressive Multifocal Leukoencephalopathy; PVS: Perivascular spaces.

PVS and sometimes age-associated WMC are to be separately considered. Involvement of U-fibers or the cortex is more often found in inflammatory or metabolic causes, although the latter are rare in adulthood.

Conflict of Interest

The authors declare that they have no conflict of interest.

References

[1] Nichtweiß M, Weidauer S, Treusch N et al. White Matter Lesions and Vascular Cognitive Impairment. Part 1: Typical and Unusual Causes. Clin Neuroradiol 2012; 22: 193–210

[2] Weidauer S, Nichtweiß M, Hattingen E. Differential diagnosis of white matter lesions: non vascular causes – part II. Clin Neuroradiol 2014; 24: 93–110

[3] Pantoni L. Cerebral small vessel disease: from pathogenesis and clinical characteristics to therapeutic challenges. Lancet Neurol 2010; 9: 689–701

[4] Pantoni L, Basile AM, Pracucci G et al. Impact of age-related cerebral white matter changes on the transition to disability – the LADIS study: rationale, design and methodology. Neuroepidemiology 2005; 24: 51–62

[5] Barkhof F, Scheltens P. Imaging of white matter lesions. Cerebrovasc Dis 2002; 13 (Suppl. 2): S21–S23

[6] Schmahmann JD, Smith EE, Eichler FS et al. Cerebral white matter neuroanatomy, clinical neurology and neurobehavioral correlates. Ann NY Acad Sci 2008; 1142: 266–309

[7] Jäger HR, Gomez-Anson B. Small Vessel Disease – Imaging and Clinical Aspects. In: Barkhof F, Jäger R, Thurnher M, et al., eds; Clinical Neuroradiology. Berlin Heidelberg: Springer; 2019: 167–201

[8] Kwee RM, Kwee TC. Virchow-Robin Spaces at MR Imaging. RadioGraphics 2007; 27: 1071–1086

[9] Rudie JD, Rauschecker AM, Nabavizadeh SA et al. Neuroimaging of Dilated Perivascular Spaces: From Benign and Pathologic Causes to Mimics. J Neuroimaging 2018; 28: 139–149

[10] Salamon G, Corbaz JM. Atlas de la vascularisation arterielle du cerveau chez l'homme. Paris: Sandoz ; 1971

[11] Eckstein C, Saidha S, Levy M. A differential diagnosis of central nervous system demyelination: beyond multiple sclerosis. J Neurol 2012; 259: 801–816

[12] Wattjes MP, Steenwijk MD, Stangel M. MRI in the diagnosis and monitoring of multiple sclerosis: an update. Clin Neuroradiol 2015; 25 (Suppl. 2): S157–S165

[13] van der Knaap MS, Bugiani M. Leukodystrophies: a proposed classification system based on pathological changes and pathogenetic mechanisms. Acta Neuropathol 2017; 134: 351–382

[14] Weller RO, Hawkes CA, Kalaria RN et al. White Matter Changes in Dementia: Role of Impaired Drainage of Interstitial Fluid. Brain Pathology 2015; 25: 63–78

[15] Rasalkar DD, Chu WC, Hui J et al. Pictorial review of mucopolysaccharidosis with emphasis on MRI features of brain and spine. Br J Radiol 2011; 84: 469–477

[16] Prodan CI, Holland NR, Wisdom PJ et al. CNS demyelination associated with copper deficiency and hyperzincemia. Neurology 2002; 59: 1453–1456

[17] Singh TD, Fugate JE, Rabinstein AA. Central pontine and extrapontine myelinolysis: a systematic review. Eur J Neurol 2014; 21: 1443–1450

[18] Blasel S, Hattingen E, Adelmann M et al. Toxic leukoencephalopathy after heroin abuse without heroin vapour inhalation: MR imaging and clinical features in 3 patients. Clin Neuroradiol 2010; 20: 48–53

[19] Geibprasert S, Gallucci M, Krings T. Addictive illegal drugs: structural neuroimaging. AJNR Am J Neuroradiol 2010; 31: 803–808

[20] Gürtler S, Ebner A, Tuxhorn I et al. Transient lesion in the splenium of the corpus callosum and antiepileptic drug withdrawal. Neurology 2005; 65: 1032–1036

[21] Bartynski WS. Posterior Reversible Encephalopathy Syndrome, Part 1: Fundamental Imaging and Clinical Features. AJNR Am J Neuroradiol 2008; 29: 1036–1042

[22] Schiffmann R, van der Knaap MS. An MRI-based approach to the diagnosis of white matter disorders. Neurology 2009; 72: 750–759

[23] Barkhof F, Fox NC, Bastos-Leite AJ et al. Neuroimaging in dementia. Berlin Heidelberg: Springer; 2011

[24] Mascalchi M, Filippi M, Floris R et al. Diffusion-weighted MR of the brain: methodology and clinical application. Radiol Med 2005; 109: 155–197

[25] Mori S, van Zijl PC. Fiber tracking: principles and strategies – a technical review. NMR Biomed 2002; 15: 468–480

[26] Bink A, Schmitt M, Gaa J et al. Detection of lesions in multiple sclerosis by 2D FLAIR and single-slab 3D FLAIR sequences at 3.0 T – preliminary results. Eur Radiol 2006; 16: 1104–1110

[27] Tatu L, Moulin T, Bogousslavsky J et al. Arterial territories of the human brain: Cerebral hemispheres. Neurology 1998; 50: 1699–1708

[28] Marinkovic S, Gibo H, Milisavljevic M et al. Anatomic and clinical correlations of the lenticulostriate arteries. Clin Anat 2001; 14: 190–195

[29] Yasargil MG. Microneurosurgery, Volume I: Microsurgical anatomy of the basal cisterns and vessels of the brain, diagnostic studies, general operative techniques and pathological considerations of intracranial aneurysms. 1. Aufl Stuttgart: Thieme; 1984

[30] Zhang ET, Inman CBE, Weller RO. Interrelationships of the pia mater and the perivascular (Virchow-Robin) spaces in the human cerebrum. J Anat 1990; 170: 111–123

[31] Weller RO, Subash M, Preston SD et al. Perivascular Drainage of Amyloid-b Peptides from the Brain and Its Failure in Cerebral Amyloid Angiopathy and Alzheimer's Disease. Brain Pathology 2008; 18: 253–266

[32] Ding J, Sigurðsson S, Jónsson PV et al. Large Perivascular Spaces Visible on Magnetic Resonance Imaging, Cerebral Small Vessel Disease Progression, and Risk of Dementia. The Age, Gene/Environment Susceptibility – Reykjavik Study. JAMA Neurol 2017; 74: 1105–1112

[33] Hachinski V, Iadecola C, Petersen RC et al. National Institute of Neurological Disorders and Stroke – Canadian Stroke Network Vascular Cognitive Impairment Harmonization Standards. Stroke 2006; 37: 2220–2241

[34] Román GC, Erkinjuntti T, Wallin A et al. Subcortical ischaemic vascular dementia. Lancet Neurol 2002; 1: 426–436

[35] Román GC, Tatemichi TK, Erkinjuntti T et al. Vascular dementia: diagnostic criteria for research studies. Report of the NINDS-AIREN International Workshop. Neurology 1993; 43: 250–260

[36] Wardlaw JM, Smith EE, Biessels GJ et al. STandards for ReportIng Vascular changes on nEuroimaging (STRIVE v1) Neuroimaging standards for research into small vessel disease and its contribution to ageing and neurodegeneration. Lancet Neurol 2013; 12: 822–838

[37] Zhu YC, Tzourio C, Soumaré A et al. Severity of Dilated Virchow-Robin Spaces Is Associated With Age, Blood Pressure, and MRI Markers of Small Vessel Disease: A Population-Based Study. Stroke 2010; 41: 2483–2490

[38] Zhu YC, Dufouil C, Soumaré A et al. High degree of dilated Virchow-Robin spaces on MRI is associated with increased risk of dementia. J Alzheimers Dis 2010; 22: 663–672

[39] Weidauer S, Wagner M, Enkirch SJ et al. CNS Infections in Immunocompetent Patients: Neuroradiological and Clinical Features. Clin Neuroradiol 2020; 30: 9–25

[40] Duering M, Csanadi E, Gesierich B et al. Incident lacunes preferentially localize to the edge of white matter hyperintensities: insights into the pathophysiology of cerebral small vessel disease. Brain 2013; 136: 2717–2726

[41] Wahlund LO, Barkhof F, Fazekas F et al. A new rating scale for age-related white matter changes applicable to MRI and CT. Stroke 2001; 32: 1318–1322

[42] van Straaten EC, Fazekas F, Rostrup E et al. Impact of white matter hyperintensities scoring method on correlations with clinical data: the LADIS study. Stroke 2006; 37: 836–840

[43] Frisoni GB, Galluzzi S, Pantoni L et al. The effect of white matter lesions on cognition in the elderly – small but detectable. Nat Clin Pract Neurol 2007; 3: 620–627

[44] Wen W, Sachdev PS. Extent and distribution of white matter hyperintensities in stroke patients: the Sydney stroke study. Stroke 2004; 35: 2813–2819

[45] Kruit MC, van Buchem MA, Hofman PA et al. Migraine as a risk factor for subclinical brain lesions. JAMA 2004; 291: 427–434

[46] Charidimou A, Boulouis G, Pasi M et al. MRI-visible perivascular spaces in cerebral amyloid angiopathy and hypertensive arteriopathy. Neurology 2017; 88: 1157–1164

[47] Greenberg SM, Charidimou A. Diagnosis of cerebral amyloid angiopathy: evolution of the Boston criteria. Stroke 2018; 49: 491–497

[48] Haller S, Vernooij MW, Kuijer JPA et al. Cerebral microbleeds: imaging and clinical significance. Radiology 2018; 287: 11–28

[49] Chabriat H, Joutel A, Dichgans M et al. CADASIL. Lancet Neurol 2009; 8: 643–653

[50] Lerman-Sagie T, Leshinsky-Silver E, Watemberg N et al. White matter involvement in mitochondrial diseases. Mol Genet Metab 2005; 84: 127–136

[51] Moore DF, Kaneski CR, Askari H et al. The cerebral vasculopathy of Fabry disease. J Neurol Sci 2007; 257: 258–263

[52] Berlit P. Diagnosis and treatment of cerebral vasculitis. Ther Adv Neurol Disord 2010; 3: 29–42

[53] Jennette JC, Falk RJ, Bacon PA et al. 2012 revised International Chapel Hill Consensus Conference Nomenclature of Vasculitides. Arthritis Rheum 2013; 65: 1–11

[54] Scolding NJ. Central nervous system vasculitis. Semin Immunopathol 2009; 31: 527–536

[55] Pollock H, Hutchings M, Weller RO et al. Perivascular spaces in the basal ganglia of the human brain: their relationship to lacunes. J Anat 1997; 191: 337–346

[56] Brownlee W, Hardy TA, Fazekas F et al. Diagnosis of multiple sclerosis: progress and challenges. Lancet 2017; 389: 1336–1346

[57] Thompson AJ, Banwell BL, Barkhof F et al. Diagnosis of multiple sclerosis: 2017 revisions of the McDonald criteria. Lancet Neurol 2018; 17: 162–173

[58] Traboulsee A, Simon JH, Stone L et al. Revised recommendations of the consortium of MS centers task force for a standardized MRI protocol and clinical guidelines for the diagnosis and follow-up of multiple sclerosis. AJNR Am J Neuroradiol 2016; 37: 394–401

[59] Wingerchuk DM, Banwell B, Bennett JL et al. International Panel for NMO Diagnosis. International consensus diagnostic criteria for neuromyelitis optica spectrum disorders. Neurology 2015; 85: 177–189

[60] Hu W, Lucchinetti CF. The pathological spectrum of CNS inflammatory demyelinating diseases. Semin Immunopathol 2009; 31: 439–453

[61] Charidimou A, Linn J, Vernooij MW et al. Cortical superficial siderosis: detection and clinical significance in cerebral amyloid angiopathy and related conditions. Brain 2015; 138: 2126–2139

[62] Roher AE, Kuo YM, Esh C et al. Cortical and Leptomeningeal Cerebrovascular Amyloid and White Matter Pathology in Alzheimer's Disease. Molecular Med 2003; 9: 112–122

[63] Salvarani C, Hunder GG, Morris JM et al. Aβ-related angiitis: comparison with CAA without inflammation and primary CNS vasculitis. Neurology 2013; 81: 1596–1603

[64] Duman IE, Coenen VA, Doostkam S et al. Teaching Neuroimages: Inflammatory CAA. Clin Neuroradiol 2019; 29: 379–382

[65] Barkhof F, Daams M, Scheltens P et al. An MRI rating scale for amyloid-related imaging abnormalities with edema or effusion. AJNR Am J Neuroradiol 2013; 34: 1550–1555

[66] Bot JC, Mazzai L, Hagenbeek RE et al. Brain miliary enhancement. Neuroradiology 2020; 62: 283–300

[67] Christoforidis GA, Spickler EM, Recio MV et al. MR of CNS sarcoidosis: correlation of imaging features to clinical symptoms and response to treatment. AJNR Am J Neuroradiol 1999; 20: 655–669

[68] Miller DH, Weinshenker BG, Filippi M et al. Differential diagnosis of suspected multiple sclerosis: a consensus approach. Mult Scler 2008; 14: 1157–1174

[69] Küker W, Gaertner S, Nagele T et al. Vessel wall contrast enhancement: a diagnostic sign of cerebral vasculitis. Cerebrovasc Dis 2008; 26: 23–29

[70] Haldorson IS, Espeland A, Larsson EM. Central Nervous System Lymphoma: Characteristic Findings on Traditional and Advanced Imaging. AJNR Am J Neuroradiol 2011; 32: 984–992

[71] Weidauer S, Wagner M, Nichtweiß M. Magnetic Resonance Imaging and Clinical Features in Acute and Subacute Myelopathies. Clin Neuroradiol 2017; 27: 417–433

[72] Kidd D, Barkhof F, McConnell R et al. Cortical lesions in multiple sclerosis. Brain 1999; 122: 17–26

[73] Susac JO, Murtagh FR, Egan RA et al. MRI findings in Susac's syndrome. Neurology 2003; 61: 1783–1787

[74] Young NP, Weinshenker BG, Lucchinetti CF. Acute disseminated encephalomyelitis: current understanding and controversies. Semin Neurol 2008; 28: 84–94

[75] Seewann A, Enzinger C, Filippi M et al. MRI characteristics of atypical idiopathic inflammatory demyelinating lesions of the brain: A review of reported findings. J Neurol 2008; 255: 1–10

[76] Mahad DJ, Staugaitis S, Ruggieri P et al. Steroid-responsive encephalopathy associated with autoimmune thyroiditis and primary CNS demyelination. J Neurol Sci 2005; 228: 3–5

[77] Akman-Demir G, Serdaroglu P, Tasçi B. The Neuro-Behçet Study Group. Clinical patterns of neurological involvement in Behçet's disease: evaluation of 200 patients. Brain 1999; 122: 2171–2181

[78] Keegan BM, Giannini C, Parisi JE et al. Sporadic adult-onset leukoencephalopathy with neuroaxonal spheroids mimicking cerebral MS. Neurology 2008; 70: 1128–1133

[79] Chang L, Shukla DK. Imaging studies of the HIV-infected brain. Handb Clin Neurol 2018; 152: 229–264

[80] Gheuens S, Wüthrich C, Koralnik IJ. Progressive multifocal leukoencephalopathy: why grey and white matter. Ann Rev Path 2013; 8: 189–215

[81] Moll NM, Rietsch AM, Ransohoff AJ et al. Cortical demyelination in PML and MS – Similarities and differences. Neurology 2008; 70: 336–343

[82] Tan CS, Koralnik IJ. Progressive multifocal leukoencephalopathy and other disorders caused by JC virus: clinical features and pathogenesis. Lancet Neurol 2010; 9: 425–437

[83] Yousry TA, Pelletier D, Cadavid D et al. Magnetic Resonance Imaging Pattern in Natalizumab-Associated Progressive Multifocal Leukoencephalopathy. Ann Neurol 2012; 72: 779–787

[84] Hodel J, Darchis C, Outteryck O et al. Punctate pattern – A promising imaging marker for the diagnosis of natalizumab-associated PML. Neurology 2016; 86: 1516–1523

[85] Lulé D, Ludolph AC, Kassubek J. MRI-based functional neuroimaging in ALS: an update. Amyotroph Lateral Scler 2009; 10: 258–268

[86] Balendra R, Isaacs AM. C9orf72-mediated ALS and FTD: multiple pathways to disease. Nat Rev Neurol 2018; 14: 544–558